UNIVERSITY OF COPENHAGEN
FACULTY OF SCIENCE
NIELS BOHR INSTITUTE

Master's Thesis

Ecosystems of Sessile Species in Inhomogeneous Environments

Markus Hofer

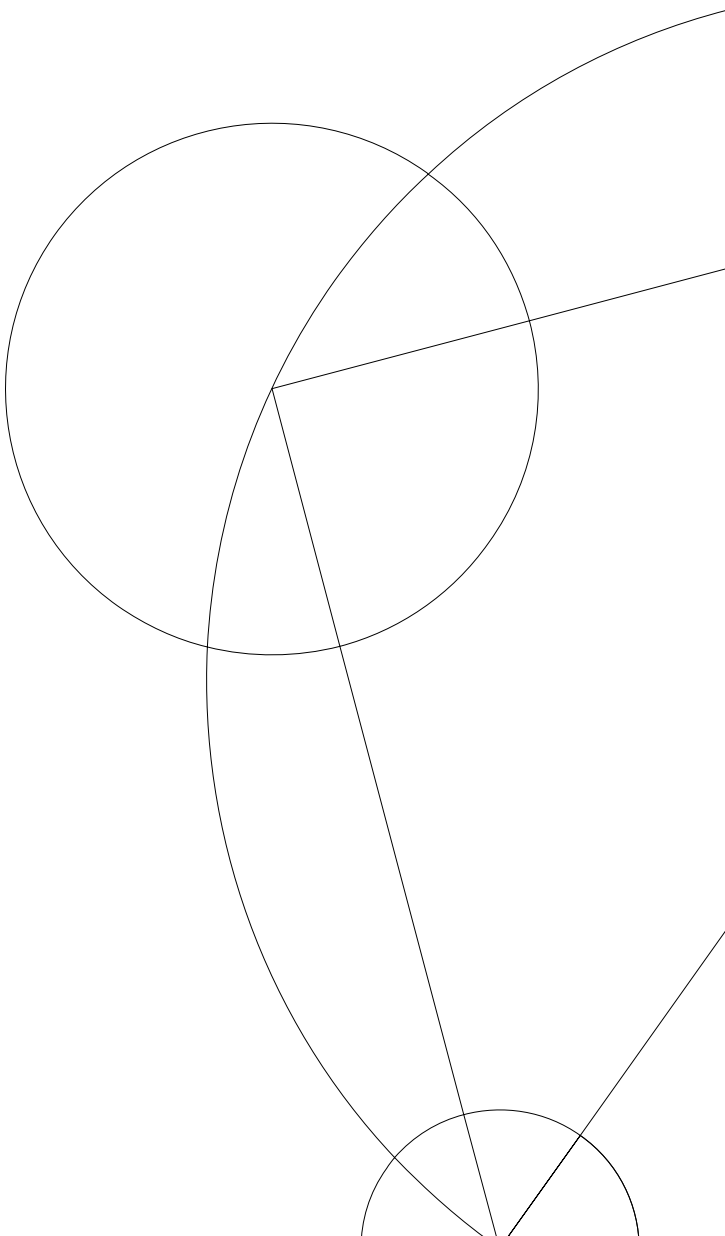

Supervisor
Kim Sneppen

May 2022

Abstract

This work considers a model of sessile species, interacting with each other according to a directed Erdős-Rényi random graph during their competition for space in a lattice. The system, first described by Mathiesen et al. [1], exhibits a first-order phase transition in diversity as the interaction probability is increased beyond a critical point. To investigate this transition from the high-diversity state to the low-diversity state further, parallel computing is used to simulate the system for a range of system sizes and interaction probabilities. For fixed interaction probabilities, the data shows that, in the high-diversity state, the number of species grows linearly with system-length. However, the slope of this growth decreases with larger interaction probability.

To investigate how inhomogeneous spatial conditions affect the model, a second interaction network is introduced to generate different update-rules based on spatial region. If the lattice is divided into two halves, one for each interaction network, the local diversity is increased at the boundary. This shows that the model exhibits edge-effects, a phenomenon of special interest in theoretical and empirical ecology [2]. Additionally, total diversity is increased and the transition between high- and low-diversity state occurs at a higher interaction probability. When the lattice sites governed by the second interaction network are placed randomly in the system, the increase in diversity and stability is much larger. This exemplifies how spatial inhomogeneity can be utilized to increase the stabilizing effect of spatial separation in model-ecosystems.

Figure 1: Colorful Lichen photographed in the Lake District of Northwest England [3].

Acknowledgements

Throughout my work on this thesis, many people have been instrumental in making my time exciting, insightful, and incredibly enjoyable. Since this project would not have been the same without them, I would like to show my appreciation here.

I would like to thank Kim Sneppen for his supervision, engaging discussions, and for sharing parts of his insight on the connection between biology and physics with me.

Furthermore, I would like to thank Namiko Mitarai and Julius Bier Kirkegaard for their help with various technical problems and the feedback they provided me with over the past few months.

I would like to thank all members of the Center for Models of Life for the engaging journal clubs, talks, and the overall amazing atmosphere at the institute.

Finally, I would like to thank my friends and family for their incredible support.

Contents

1 Background **1**

1.1 Lotka-Volterra Systems 2

1.2 Random Matrix Approach for Large Ecosystems 4

1.3 Probabilistic Cellular Automata 6

1.4 Buss-Jackson-Karlson–Model 8

2 The Sessile Species Model **10**

2.1 History 11

2.2 Space, Species and Interactions 12

2.3 Updating-Schemes 13

2.3.1 Local Updates 13

2.4 Acceleration of Cyclic Interactions 15

2.5 Stochastic and Cyclic Patch Creation 16

2.6 Choice of Time-Measurements 20

3 Implementation **21**

3.1 Technical Overview 21

3.2 Speed Comparison Between Sequential and Parallel Implementation . 22

3.3 Differences between Sequential and Parallel Implementation 22

4 Results & Discussion **26**

4.1 Generation of Initial Conditions 27

4.2 Building Stable High Diversity States 28

4.3 Average Diversity & Number of Patches for $n_{intro} = 2$ and $n_{intro} = 1$. 30

4.4 Species Size Distribution 33

4.5 Patch Size Distribution 35

4.6 Distribution of Time between Static States 36

4.7 Lower Limit of Stable System Sizes 37

4.8 Comparison of System Sizes 39

4.9 Ecosystems with Inactive Lattice Sites 42

4.10 Split Ecosystems 44

4.11 Random Condition Ecosystems 47

4.12 Removal of Cyclic Interactions 50

5 Conclusions **52**

5.1 Effects of System Size 52

5.2 Effects of Inhomogeneous Spatial Conditions 52

6 References **54**

7 Appendix **58**

1 Background

To better understand and appreciate the models discussed in the later sections, it is beneficial to gain a preliminary understanding of various other models in theoretical ecology first. As such, the following sections (Lotka-Volterra Systems (Section 1.1) and Random Matrix Approach to large Ecosystems (Section 1.2)) introduce approaches used in modeling ecosystems. While the models discussed are important and interesting on their own, they are chosen here as they exemplify an underlying theme present in parts of theoretical ecology: Attempts at describing large ecosystems mathematically often result in instability of the system. This idea is often referred to as the *stability-complexity trade-off*. In the examples of Lotka-Volterra Systems and May's random matrix approach, this is quantified in the instability of arbitrary states, as determined by local stability analysis.While discussing random matrix models of large ecosystems, a common remedy for this instability problem is introduced through another example: The introduction of space (or more specifically, spatial separation between species) can significantly improve the stability of the system.

In preparation of further models, probabilistic cellular automata are introduced and one deterministic example is displayed. However, it is only meant to illustrate the concept of cellular automata and is not directly related to further discussed models. Following the introduction of the two important concepts of the complexity-stability trade-off and possible stability improvement through spatial separation, research from Buss, Jackson and Karlson is discussed, as it could be viewed as a precursor to the models discussed in the main part of this thesis.

The model defined by Jackson and Karlson and the later discussed sessile species model are based on probabilistic cellular automata. This change from the differential equation models in sections 1.1 and 1.2 allows for significantly better modeling of spatial separation. As a result these models tend to be more stable. This motivates a different approach to classifying the system's stability. Rather than considering the stability of an arbitrary state, special emphasis is placed on the stability of states with multiple species coexisting at the same time. As result the diversity D

$$D(S) = \sum_{\text{species } i} \mathbb{1}\{i \text{ alive in } S\} \tag{1}$$

becomes one of the most important metrics of the system S. Where $\mathbb{1}$ is the indicator function following a simplified definition $\mathbb{1}\{x\} = 1$, if condition x is fulfilled and 0 otherwise.

1.1 Lotka-Volterra Systems

Although initially intended for chemical reactions by Lotka in 1920 [4], the equation system

$$\frac{dN}{dt} = N(a - bP) \tag{2}$$
$$\frac{dP}{dt} = P(cN - d) \tag{3}$$

in now mostly known for its application to fish populations in the Adriatic Sea by Volterra in 1926 [5, 6]. Following Volterra's interpretation, $N(t)$ is the population of prey-fish, $P(t)$ is the population of predator-fish, and a, b, c, and d are positive constants. In order to show how these so-called Lotka-Volterra systems and their extensions for k prey-species and k predator-species lead to instabilities, the arguments from Murray [7] are summarised below:

2 Species Lotka-Volterra System

Equations (2) and (3) can be brought to the dimensionless form

$$\frac{du}{d\tau} = u(1 - v) \qquad \frac{dv}{d\tau} = \alpha v(u - 1) \tag{4}$$

With

$$u(\tau) = \frac{cN(t)}{d}, \qquad v(\tau) = \frac{bP(t)}{a}, \qquad \tau = at, \qquad \alpha = \frac{d}{a}. \tag{5}$$

The resulting trajectories in phase-space follow the differential equation

$$\frac{dv}{du} = \alpha \frac{v(u-1)}{u(1-v)} \tag{6}$$

with solution

$$\alpha u + v - \ln u^{\alpha} v = H, \tag{7}$$

where H is determined through the initial conditions $u(0)$ and $v(0)$. The equation system (4) has two singular points, $(0, 0)$ and $(1, 1)$. Linear stability analysis at these points reveals that $(0, 0)$ is linearly unstable, while solution in the neighbourhood of $(1, 1)$ are periodic with period $T = 2\pi\sqrt{\alpha}$.

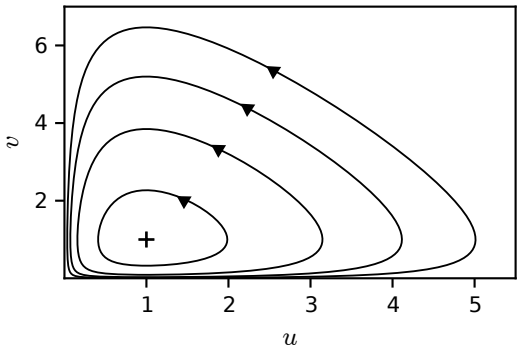

Figure 2: Trajectories in the (u, v)-phase space for 4 values of H. Arrows indicate the direction on the trajectories.

2k Species Lotka-Volterra System

Extending the Lotka-Volterra equations (2) and (3) for k prey-species and k predator-species leads to

$$\frac{dN_i}{dt} = N_i \left[a_i - \sum_{j=1}^{k} b_{ij} P_j \right] \tag{8}$$

$$\frac{dP_i}{dt} = P_i \left[\sum_{j=1}^{k} c_{ij} N_j - d_i \right], \tag{9}$$

with a_i, b_{ij}, c_{ij} and d_i being positive constants and $i \in \{1, \ldots, k\}$. Similar to the 2 species case, the trivial steady state $N_i = P_i = 0$, $i \in \{1, \ldots, k\}$ is unstable.
Solutions for the nontrivial steady-state $(\vec{P}^*, \vec{N}^*)$ require

$$B\vec{P}^* = \vec{a}, \qquad C\vec{N}^* = \vec{d}, \tag{10}$$

with $\vec{a}, B, C$ and $\vec{d}$ being the matrices and vectors according to a_i, b_{ij}, c_{ij} and d_i respectively.
Linearization of the systems dynamics at $(\vec{P}^*, \vec{N}^*)$ leads to,

$$\begin{pmatrix} \frac{d\vec{u}}{dt} \\ \frac{d\vec{v}}{dt} \end{pmatrix} \approx A \begin{pmatrix} \vec{u} \\ \vec{v} \end{pmatrix}, \qquad A = \left(\begin{array}{c|c} 0 & -\vec{N}^{*T} B \\ \hline \vec{P}^{*T} C f & 0 \end{array} \right). \tag{11}$$

With A being referred as the community matrix in mathematical biology.
Due to its structure, A must satisfy.

$$\sum_{i=1}^{2k} \lambda_i = \text{tr}\,(A) = 0. \tag{12}$$

This leads to two possible options. Either $\Re(\lambda_i) = 0$ for all i, leading to a neutrally stable steady-state. If this is not the case, due to (12), at least one i exist such that $\Re(\lambda_i) > 0$ and the resulting state is in-stable.
In result, one could form the intuition that as k increases, stable states are less likely in the $2k$ Lotka-Volterra system. Or in the words of J.D. Murray: *"complexity usually results in instability rather than stability"*[7].

1.2 Random Matrix Approach for Large Ecosystems

In order to give more credibility to the intuition developed in the previous section, it is useful to consider May's random matrix approach to large ecosystems. Following a hypothesis developed by Gardner and Ashby [8], based on insight from their simulations, May developed a mathematical model describing the possibility of stability for large ecosystems [9]. This argument is presented following [10]:
The community matrix A is not structured as the ones in the previous section were. Instead, A is an element of a random matrix ensemble with the following characteristics:

1. Off-diagonal coefficients of A are 0 with probability $1 - C$. If this is not the case (with probability C), they are sampled independently from a distribution with mean 0 and variance σ^2. These elements model random integration between species.

2. Diagonal coefficients are set to $-d$, $d \in [0, \infty)$, representing the amount of self regulation every species has.

This assumption conveniently eliminates the need for knowledge of the ecosystem's dynamics. While this is obviously a large assumption to make, considering that no commonly accepted set equations modeling the behavior of species in an ecosystem exist, it provides a starting point for further analysis. Additionally, the random interaction assumption allows for the distribution of eigenvalues to be determined analytically through random matrix theory.

For this it is useful to first consider the eigenvalue distribution of a non-symmetric random matrix ensemble:

First define the eigenvalue distribution itself as

$$\mu(\lambda) = E\left(\frac{1}{n}\sum_{i=1}^{n}\delta\left(\lambda - \lambda_i\right)\right). \tag{13}$$

Where λ_i are the eigenvalues, E is the expectation in respect to the entire ensemble of random matrices and δ is the Dirac δ-function. Furthermore it is helpful to define the so called *resolvent* $G(z)$.

$$G(z) = E\left(\frac{1}{n}\sum_{i=1}^{n}\frac{1}{z - \lambda_i}\right) = E\left(\frac{1}{n}\operatorname{tr}(z1 - A)^{-1}\right) \tag{14}$$

Which allows the computation of the spectral density through

$$\mu(\lambda) = \frac{1}{\pi} \lim_{\epsilon \to 0^+} \operatorname{Im} \mathcal{G}(\lambda + i\epsilon) \tag{15}$$

For a non-symmetric $n \times n$ random matrix M with all coefficients m_{ij} being iid. random variables with $E[m_{ij}] = 0$ and $E[m_{ij}^2] = 1$ then $\mu(\lambda)$ of $M/\sqrt{n}$ converges to

$$\mu(\lambda) = \begin{cases} \frac{1}{\pi} & \text{if } (\Re(\lambda))^2 + (\Im(\lambda))^2 \leq 1 \\ 0 & \text{otherwise.} \end{cases} \tag{16}$$

as $n \to \infty$.

From this result one can obtain the radius of eigenvalues for the random community matrix defined by May. If A is re-scaled by $\sqrt{C\sigma^2}$, the resulting matrix $A/\sqrt{C\sigma^2}$ has the same characteristics as M. Therefore the radius of $A/\sqrt{C\sigma^2}$ converges to 1 as $n \to \infty$. In order for the system remain in a stable state, the diagonal elements of the community matrix have to remain negative. This leads to the so-called May's stability criterion

$$\sqrt{nC\sigma^2} < d. \tag{17}$$

Similar to the intuition obtained from the $2k$-species Lotka-Volterra system in the previous section, May's stability criterion indicates that large systems sizes n and high connectivity C are incompatible unless significant self regulation d is present in the system.

Meta-Community Ecosystems

As highlighted by the examples of the $2k$-species Lotka-Volterra systems and May's stability criterion, large ecosystems should be less stable from a mathematical viewpoint. This is commonly referred to as the complexity-stability paradox. However, when actual observations are considered, real ecosystems are obviously not effected by this complexity-stability trade-off to the same extent. This discrepancy led to the development of multiple hypothesis. While no explanation has been commonly accepted so far, a relevant contender is the introduction of spatial separation into the system.

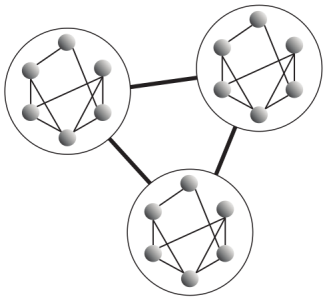

Figure 3: Schematic of a Meta-Ecosystem from [11] representing 3 connected sub-ecosystems.

As is discussed in [11], with a modification of the community-matrix structure, the

stability criterion (17) can be significantly relaxed. Instead of considering only a single ecosystem, a network of connected sub-ecosystems is constructed. Individual sub-ecosystems follow the definition of May. In the meta-ecosystem, all k sub-ecosystems are connected, as one assumes that there is species-dispersal between them. The community matrix of the connected system is of shape $(nk \times nk)$, where n is the number of species in the system. Both numerical as well analytical investigations show that an increase in the number of sub-ecosystem increases the system's stability.

1.3 Probabilistic Cellular Automata

As shown by the example in the precious section, the introduction of space can lead to an increase in stability of the overall ecosystem. This allowed the initially diversity-averse May-random-matrix model to increase in stability once spatial separation through the introduction of multiple connected sub-ecosystems was introduced. This effect can be seen in various other model-ecosystems [12]. While the spatial separation in the previous section was based on differential equations, using cellular automata can lead to an arguably better separation between species and result in stabler system states.
This expectation is used in the main focus of this thesis, the sessile species model (described in sections 2.2, 2.3 and 2.5). Therefore it is useful to give a brief description of*cellular automata* and *probabilistic cellular automata* to make the introduction of the sessile-species model more accessible to the general reader. Further information can be found in [13]

Cellular Automata (CA) consists of a set of finite-state automata (referred to as cells), which are arranged in a lattice. The change in cell-state for any cell i from any t to Δt only depends on the cell-state of i and the states of its neighbors. Widely known papers involving CA include the 1948 paper by von Neumann and Ulam [13], usually considered the first mention of CAs, and Conway's Game of Life [14], due to the variety of structures it can form.

Example: Rule 30 CA [15]

In figure (4) every square represents a cell. The cell's state is indicated by its color. White cells are active, black one passive. The state of a cell and it's two nearest neighbors at t determines the state of the cell at $t+1$. If black cells are assigned the number 0 ad white cells the number 1, the combination of the $t+1$-rows (left to right, top to bottom), reads 00011110. This is the binary representation of 30 in decimal representation.

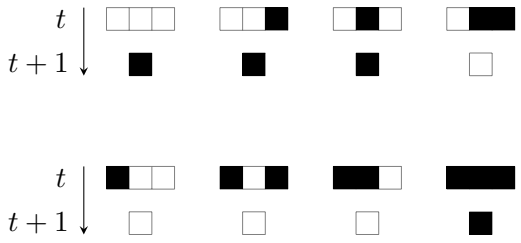

Figure 4: Schematic of all dynamics in Rule 30.

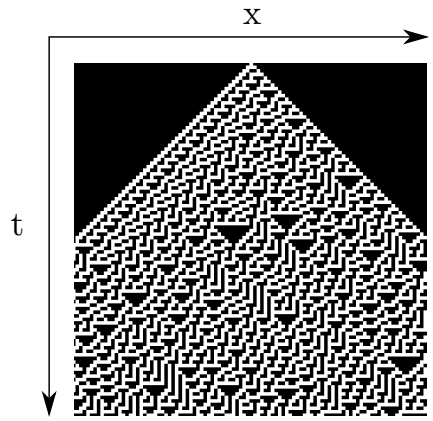

Figure 5: Simulations of Rule 30. Starting from a single active cell.

Probabilistic Cellular Automata (PCA) extend the definition of cellular automata by allowing the introduction of randomness into the update rule for cell-states. This can be done either through randomness in the set of rules describing the evolution of cells state based on its and its neighbor's states, or by only updating a random subset of cells every timesteps.

Since the update for every cell only requires knowledge of its state and the states of its neighbors, a large number of cells can be updated simultaneously with interfering with other updated cells. This allows for excellent parallelization.

Due to their flexibility and relative ease of implementation, PCA have been used in a variety of fields including: epidemiology [16], voting/opinion dynamics [17] and traffic models [18].

As described later the main focus of this thesis, the sessile-species model is best described as a partially asynchronous stochastic cellular automaton.

1.4 Buss-Jackson-Karlson–Model

In 1975, based on studies of limit-cycle studies of the Lotka-Volterra system for three or more species, it was hypothesised that intransitive competition relationships could lead to coexistence between species [19]. In the same year, proof of such relationships was found in a bay in northern Jamaica [20]:

The observed reef was inhabited by various corals and sponges. Relative competitive strength between species in the ecosystem was determined through the overgrowth between species. This means that if species A was found to grow on top of species B, as such taking over species B's place on the reef-substrate, species A was assumed to be competitive dominant when compared to species B. Over a long enough period and without other interruptions, species A should have completely overtaken the adjacent patch of species B on the reef-substrate.

Following the discovery of ecosystems inhabited by species with intransitive competition behaviors, computational models were developed to gain a deeper understanding of the processes maintaining stability and diversity in the system. Mimicking the studied corral-reef, the individuals in the model ecosystem were assumed to be sessile. The models simulated by Karlson and Jackson [21], and analyzed further by Buss [22], try to implement the growth of coral and sponges on a small two-dimensional lattice. These models will be referred to as *BJK-model*.

	C_4	C_3	C_4					D_4	
C_4	C_3	C_2	C_3	C_4			D_4	D_3	D_4
C_3	C_2	C_1	C_2	C_3	C_4			D_4	
A_3	C_3	C_2	C_3	C_4					
A_2	A_3	C_3	C_4				A_4		
A_1	A_2	A_3	A_4						
A_2	A_3	A_4			B_4				
A_3	A_4			B_4	B_3	B_4	D_4		
A_4					B_4	D_4	D_3	D_4	
							D_4		

Figure 6: Hypothetical example of a Buss-Jackson-Karlson-Model on a 10×10-lattice, showing the interaction between 4 species $\{A, B, C, D\}$. Subscripts denote in which interval the lattice site was recruited by its current species. Bold lines indicated contact between species. Depending of the interaction-structure overgrowth might be possible. Recreated from a similar example in the original paper [21].

Interactions between individual species in the BJK-model are defined explicitly to either form a hierarchical structure, a simple network or a complex network. Following the definitions in

[21]: in the hierarchical version a species with high rank is allowed to take over any species with lower rank. The simple network is achieved from the hierarchical structure through allowing one species with low rank to take over a species with high rank. As a result the interaction-network has one cycle. For the complex network more cycles are added to the interaction-network. Other than these mentioned ranking patterns, the systems' evolution depends on recruitment rates, growth rates, over-growth rates, substratum size (i.e., size of a spatial array), and number of species. When measured by their diversity, systems with complex networks performed best. Systems with the simple network still achieved a higher diversity than the pure hierarchical version.

In contrast to the previously noted models, the BJK model exhibits multiple fundamental changes. As the model consists of stochastic cellular automata, linear stability analysis is no longer applicable. The discussed theories however remain of some use, when thinking about the mean field approximation of the BJK-model. In result, developed intuitions might still apply here.

2 The Sessile Species Model

The following section introduces previous research on a model ecosystem consisting of species with random interactions. The system's dynamics and possible effects thereof are described in detail. Since there are minor differences between the sequential and parallel implementations of the model, the description of the system's update rules is split into *local updates* (which are identical for the sequential and parallel implementation) and the *selection-scheme* determining which lattice sites should be updated. This choice of selection-scheme is the only difference between sequential and parallel implementations.

Following the introduction of the system's dynamics, the acceleration of cyclic interactions is discussed as a method to significantly decrease simulation time. Afterwards, it is discussed how some immediate consequences of the system's rules effect diversity and overall structure of the system. Finally, some example states for the system are displayed.

Figure 7: From [1]: "Photograph of a crustose lichen community on a rock in an alpine environment (at 1300 m altitude, Jotunheimen, Norway)"

Due to the large amount of data generated it was necessary to sub-sample the generated states. In section 2.6 the choice of how the data should be sub-sampled is discussed.

For the remainder of this thesis the model described in the following sections will be referred to as the *Sessile Species Model* and shortened to the acronym *SSM*. To differentiate between the SSM and its modifications introduced later, modified versions will be described with a fitting adjective (i.e. inactive SSM), whereas SSM will refer to the unmodified version. Furthermore, unless otherwise mentioned, SSM refers to the parallel implementation (discussed in section 2.3) specifically.

2.1 History

Partially building on results from BJK-model Mathiesen, Mitarai, Sneppen, and Trusina introduced a model of sessile species in 2011 [1]. The overall evolution of the system was simplified: recruitment rates, growth rates, and over-growth rates are identical for all species. Where Jackson and Karlson tried to model coral and sponges, Mathiesen et. al. took crustose lichen as their biological motivation for the model. An example image from the original paper is displayed in figure (7).

Comparing the BJK-model to the SSM, assumptions regarding the structure of species-interactions were relaxed, as it was assumed that species interactions form a Erdös-Renyi $G(n, \gamma)$ random network. As such the system is not restricted by the choice between hierarchical interaction networks and those with circles.

Furthermore, the number of species in the system was allowed to increase, whereas in the BJK-model it was only possible to decrease D. In the SSM, additional species were introduced throughout the simulation both with a constant random rate α, or whenever all dynamics in the system were stopped (i.e. when no cell could take over its neighbors). In the original paper simulations with $\alpha = 0$ were referred to as *quasi-static* simulations. These simulations will be the main focus of this thesis.

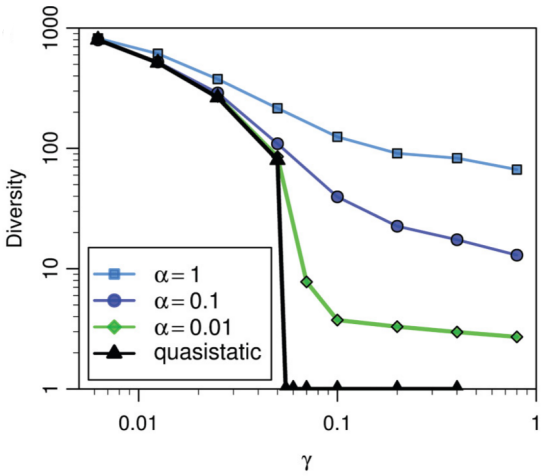

Figure 8: Plot from [1] displaying the phase-transition for a system of size 200×200. Connecting lines are drawn to guide the eye.

Depending on γ the diversity of system shows a clear phase transition between a high diversity state with $\gamma < \gamma_c$ or a low-diversity state with $\gamma > \gamma_c$. However, high introduction rates for new species increase the diversity for $\gamma > \gamma_c$. As a result, the phase transition is less visible for systems with high introduction rates.

In [23] further investigation of the SSM were conducted. To study the effect of cyclic interactions, all cycles of length σ were removed from the interaction network $G(n, \gamma)$. In contrast to the models of Jackson and Karlson, this increased the diversity for all $C_{\min} <= 5$. For $C_{\min} > 5$ diversity however decreased significantly.

In 2014 a modified version of the model, with random species introduction being replaced by the mutation of species, was published [24]. However, the structures formed by the competing species were long-lasting enough to allow any given species to significantly mutate before invading its neighbor. As such, the mutation-model behaves similarly to its predecessor with new species being added through immigration.
Further investigations were conducted, focusing on high introduction rates α and higher interaction probabilities, for the first time making use of parallel computation to accelerate simulations [25].

2.2 Space, Species and Interactions

The implemented model mimics a ecosystem of sessile species with local interactions: On a square $L \times L$ lattice with closed boundaries, every cell can be occupied by only one species at a time.

Species
Every species is fully characterized by:

- species index $s \in \mathbb{N}$
- interactions with other species as defined by the interaction network Γ

$$\Gamma_{i,j} = \begin{cases} 0 & \text{if } i = j \\ 1 & \text{with probability } \gamma \\ 0 & \text{else} \end{cases} \tag{18}$$

Interaction–Network Γ
The interactions between species form a directed network. In order to limit assumptions about the overall structure of the network, the network is defined as a directed random network. Every species is represented by a node. Competitive dominance is indicated by a (directed) edge in the network.

Every species is assumed to be competitively dominant to another any species with probability γ. As a result, the network is a directed Erdős-Rényi network. For practical purposes, it is sometimes useful to consider the adjacency matrix of said network.
Since the state of the SSM would not change if a lattice-site would invade a neighbor of the same species, self-loops in the interaction-network are forbidden. Following, the diagonal of the interaction-matrix, defined in (18), only consist of zeros. Throughout this thesis the interaction network and its matrix representation will be used interchangeably. For reference, sponge-corral, an example for a real sessile ecosystem, has been reported to compete with a 2.5% chance [26].

2.3 Updating-Schemes

Throughout the previous studies, multiple ways of updating the system have been utilized. While the *local updates* are the same in all of them, differences exist in the selection of lattice-sites (referred to as the *selection-scheme*). As a result, the local update rules are introduced separately, followed by two methods of selecting the sites where updates occur.

Since one local update only has a minor impact on the system, it is useful to define *lattice-updates* (sometimes simply referred to as *updates* or *time-steps*) as the combination of $L \times L$ local updates. On average every cell in the lattice should be active once during a lattice-update.

2.3.1 Local Updates

A local update-steps starts with a selected lattice-site (i, j). One of the four neighbors in its Von-Neumann neighborhood is chosen at random. If the species at the selected site (i, j) is dominant in comparison to the species of the chosen neighbor site, the neighboring lattice site changes to the species $s(i, j)$. If the species at the selected site (i, j) is not dominant in comparison to the neighboring species, no change takes place.

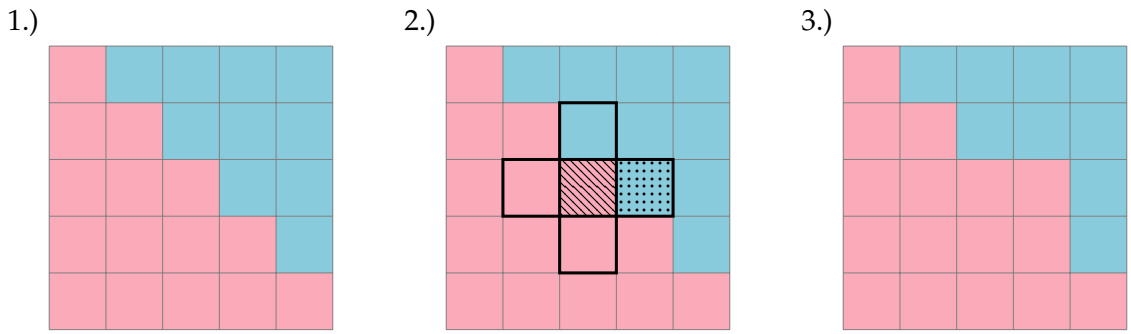

Figure 9: Schematic of a local update-step: $1.)$ Initial state. The red species is presumed to be competitive dominant to the blue species. $2.)$ A cell is selected. (black lines) And one of its 4 neighbours is randomly chosen. (dots) $3.)$ The neighboring cell changes species.

Sequential-Selection-Scheme

Only one lattice site (i, j) is chosen at a time for the sequential-updating scheme. The selection of the lattice site is random and uniform over the entire lattice. Local dynamics then take place between the selected site and one of its neighbors according to local update rules. Once this process is completed, a new lattice site is chosen.

Parallel-Selection-Scheme

In the parallel version of the updating scheme, $N/8$ lattice sites are active at the same time. In order to guarantee that no lattice-site is being invaded by two species at once, the following selection method was implemented:

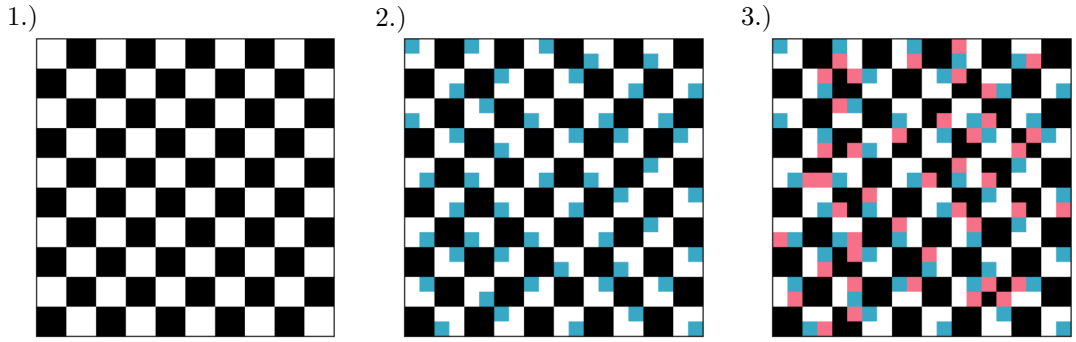

Figure 10: Example of parallel selection: 1.) active (white) and passive (black) blocks are selected 2.) One defending cell (blue) is chosen per active block. 3.) Every defending cell is assigned an adjacent attacking cell (red). Some attacking cells are outside the displayed area.

2×2 - blocks in the lattice are designated as either *active* or *passive*, following a chessboard pattern. This layout switches randomly to ensure that every site is active and passive for equally many updates. In every active block, one lattice site is chosen as the defending species. Every defending lattice site is assigned one corresponding attacker out of its 4 neighbors. With defending and attacking cells chosen, the local updates start.

To implement this selection-scheme and utilize parallel updates, the lattice-length L has to be a multiple of 4. All simulated system-sizes are selected accordingly.

2.4 Acceleration of Cyclic Interactions

As already noted in [23], cyclic interactions between species can significantly increase the number of lattice-updates needed for the system to reach a static state. While occurrence of such cyclic interactions can impact the diversity and structure of system, the length of the occurrence should only play a secondary role. Therefore, it is beneficial to stop cyclic interactions after a certain time τ_{limit} has passed. The exact procedure for this is as follows:

If the system is not stationary after τ_{min} lattice-updates since the last species has been introduced, it is determined which species currently have neighbors they can invade. Out of these species one is chosen randomly and all its edges in Γ indicating competitive-dominance over another species removed. Therefore a cyclic interaction containing this species will be hierarchical and will stop after a short time. In case this does not have the desired effect, the procedure is repeated every τ_{limit}. After the system reaches a stationary state all removed interactions are introduced again.

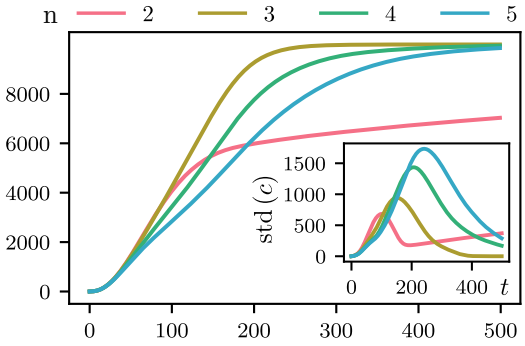

Figure 11: Average number of lattice sites that were in contact with a specific species. Data based on simulations of n species on a 100×100 lattice. Due to the circular interaction network, all species in a system are equal and results are averaged over all n species. 1000 simulations were conducted for every choice on n. Systems that did not have an active cyclic interaction after 500 lattice updates were discarded. Initial states were randomized for every simulation.

As can be seen in figure (11), an area occupied by 3 or more cyclically interacting species quickly results in every species occupying every lattice site temporarily. Therefore, every patch neighboring this area has a chance to interact with all species inside the area before the cyclic dynamics halt. If this well mixed state is achieved and no neighboring patch interacts with the species inside the area, there should be no consequence for stopping the cyclic dynamics. Cyclic interactions between only 2 species mix noticeably slower. However, it appears there is not significant effect on the diversity if instead of this cyclical interaction a hierarchical on is created.

The dynamics displayed in figure (11) were simulated on a 100×100 lattice. Based on [23] and results discussed further below, this lattice area could be viewed as an approximate upper bound for the sizes of observed patches. As such the simulated 500 steps should serve as a rough estimate for time needed to interact with all lattice sites adjacent to the specified area. More complex patch shapes could influence this estimate. In [23], even a lower τ_{limit} of 4×10^3 caused no significant change in average diversity. However the simulations discussed in the paper were carried out with $\tau_{\text{limit}} = 4 \times 10^4$. For all simulations in this thesis, a threshold of τ_{limit} of 1×10^4 was used.

2.5 Stochastic and Cyclic Patch Creation

Based on the previous research and after introducing the details of the SSM, it is possible to discuss mechanism running on larger time and length scales. These mechanisms, named *stochastic patch creation* and *cyclic patch creation*, play a significant role in understanding how diversity is created [1].

Stochastic Patch Creation

As already noted in the initial paper about the SSM [1], one of the mechanisms presumably responsible for the creation of diversity is the so-called stochastic patch creation. In its simplest form, stochastic patch creation happens during the interaction between three species with linear interactions between them. This means that species $1 \to 2 \to 3$, where the numbers represent species and arrows edges in the interaction network.

An example of this is shown in figure (12). Obviously stochastic patch creation can happen multiple times with each introduction of a new species. This by itself does not increase diversity. But when multiple (disconnected) patches of the same species are present in the system, one of the patches can be selected for the introduction of a new species, while the other patches remain unchanged, ultimately increasing the diversity.

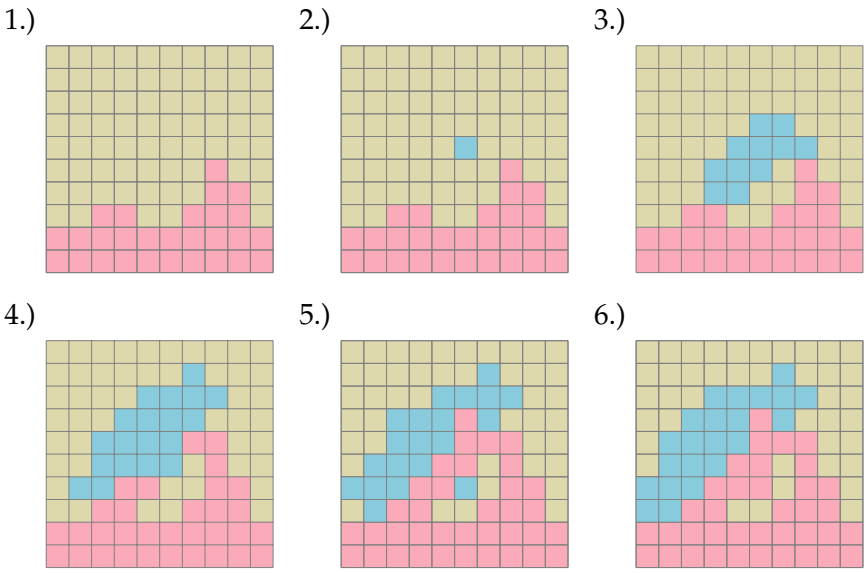

Figure 12: Example for stochastic patch creation. 1.) Species A (yellow) and species B (red) cannot invade each other. 2.) The system is stationary and as a result a new species C (blue) is introduced. 3.) After species C has spread through some of the area occupied by species A, species C comes into contact with species B. 4.) Species C continues to spread into species A, while simultaneously being overtaken by species B. 5.) Species B separates a small area containing species A and C. 6.) Species B finished invading species C inside that small area, leaving two protected patches of species A.

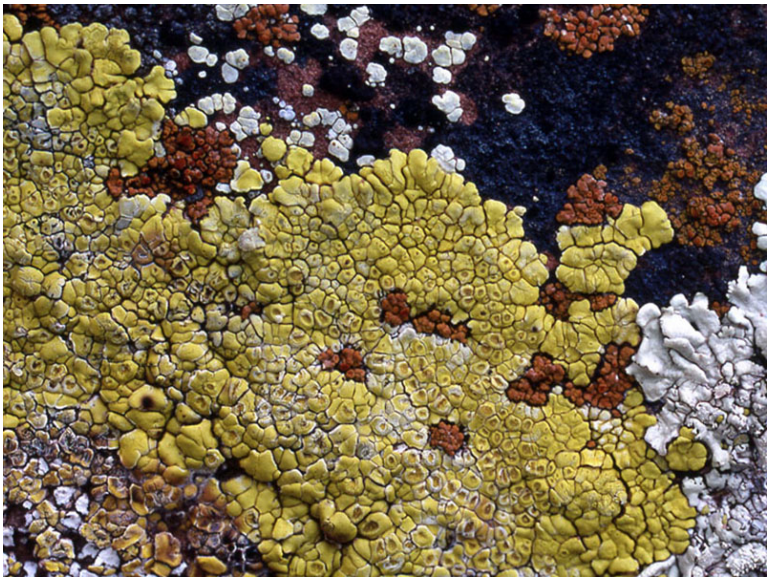

Figure 13: Photograph of Pleopsidium Flavum [27]. Some red species patches are completely surrounded by the yellow species. As a result, they could be protected from other species, i.e. the white species.

Cyclic Patch Creation

When a cyclic interaction starts with 3 or more species starts ($A \to B \to C \to \ldots \to A$), the number of patches increases significantly in a short amount of time. As has already been noted in [23], when these interactions finally break down, the leave some patches behind.

This can lead to a significant increase in the number of patches in the whole system. Statistics about the number of remaining patches and the time needed until the system naturally collapses are shown in figure (14):
To investigate the effect of cyclic interactions further, a modified version of the SSM was considered in [23]. There, for every new species, interactions were suggested according to the standard definition of the interaction matrix Γ in equation (18). If any of these interactions would lead to the creation of cycle of length less than C_{min} in the interaction network, the suggestion was discarded. This process repeats until suitable interactions are found.

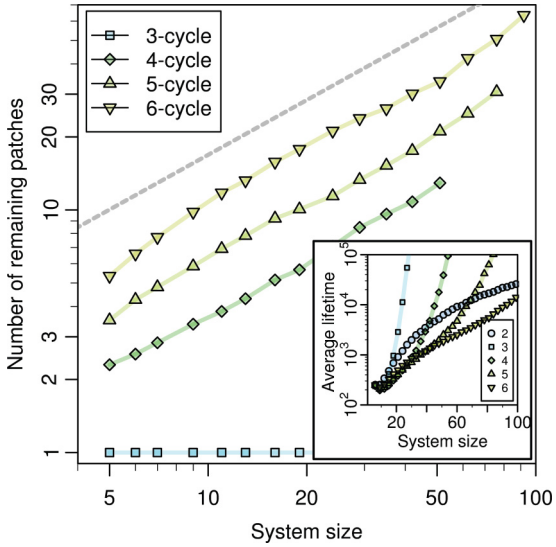

Figure 14: From [23]: "Investigation of breakdown of cycles: Average number of patches that are left when cycles of length $3, 4, 5$, and 6 collapse due to fluctuations associated with the stochastic update of the system. The dashed line corresponds to the scaling $P \propto L^{0.75}$. The inset shows the average lifetime of the cycles of length $2, \ldots, 6$ as a function of system size."

The values of C_{min} where chosen between 3 and 11. Additionally, data from the unmodified SSM can be considered for the $C_{min} = 0$ case. Simulations were initiated from a state of high diversity, generated with random introduction rate $\alpha = 0.025$ and $\gamma = 0.5$. The two cases $\gamma = 0.025$ and $\gamma = 0.05$ were considered.

Figure (15) shows the diversity of quasistatic states for various C_{min}. The notation ≥ 3 denotes that $C_{min} = 3$, and as such, only cycles of length 3 or larger can be present in the interaction network. Figure (15) would indicate that removing cycles up to $C_{min} = 5$ from the interaction network, increases the diversity. Whereas the removal of larger cycles causes the system to collapse to its low diversity state. Therefore, one could assume that cycles of length $4 - 6$ are vital in the creation of patches and as such for the diversity of the system. This idea is revisited later in section 4.12.

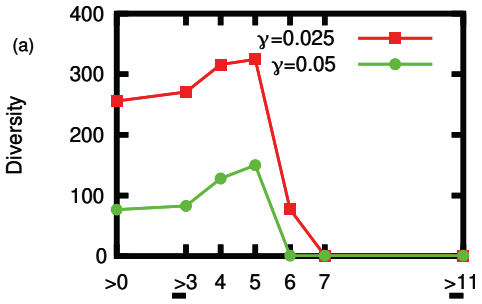

Figure 15: From [23]. Steady state diversity in a model ecosystem with the removal of short cycles.

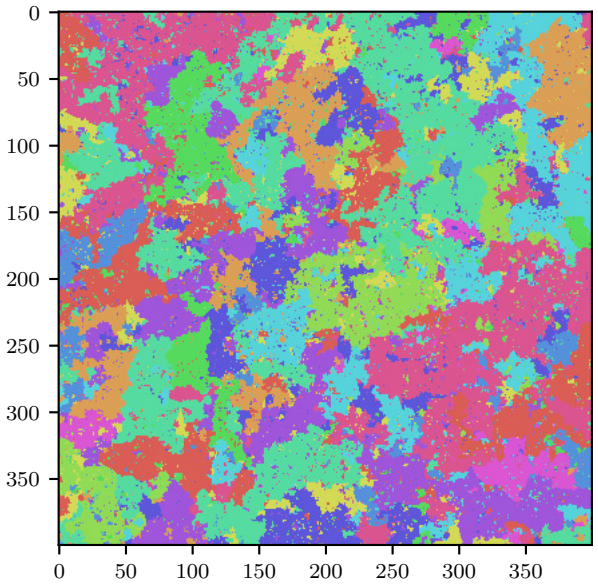

Figure 16: Example static state of a system with size 400×400 and $\gamma = 0.05$, after 7000 static states. For the first 5000 static states, two species were introduced if the systems was stationary.

2.6 Choice of Time-Measurements

For practical purposes it was necessary to only save a subset of the generated data, as storing every time-step would have significantly exceeded the storage capacity. Given this limitation, one must make a choice on which states to sample. Two options were considered:

1. *Equidistant Time Sub-sampling*
   In this sampling mode, states are sampled every n time-steps. In the preliminary tests $n = 1000$ was chosen.

2. *Static State Sub-sampling*
   In static state sub-sampling, states are only recorded whenever all local dynamics in the system are stopped (when no cell can invade its neighbors).

In the initial comparisons between both sub-sampling-methods, multiple statistics like number of patches or patch size were less noisy in the static state sub-sampling mode when sampled at an equidistant number of sub-static states. This can be attributed to transient dynamics being recorded in the equidistant time sub-sampling mode. Especially cyclic dynamics could significantly increase the number of patches and in turn add many small patches. Static states are in part immune to recording such fluctuations.
Furthermore, one could argue that there are long stretches of time between the introduction of new species in a real ecosystem. If this is the case, the introduction of a new species to the system would be followed by a comparatively brief period of activity, followed by an extended period of the system being completely static. As a result, one might be more likely to encounter a static state in real ecosystems. A similar argument is already presented in [23], where it is also assumed that in real ecosystems there are long periods of time between the introduction of new species, and as such, the quasi-static simulation might be more relevant that the case with $\alpha > 0$.
Taking the reduced noise and the possibility of better interpretation into account, static state sub-sampling was chosen as the main sub-sampling mode. Therefore, unless it is explicitly specified, all data is collected with static state sub-sampling.

3 Implementation

3.1 Technical Overview

In order to keep an easily maintainable code-base, Python was chosen as the main programming language of this project. The GPU machine-code was generated through the Numba package [28]. While earlier versions of Numba were supposed to work on both Nvidia Cuda GPUs as well AMD ROCm GPUs, the current status of the package for AMD graphics-cards is *unmaintained*[29]. Additionally, as only Nvidia graphics-cards were available, it is highly unlikely that implementation is functional on AMD GPUs.

Name	Version
Linux-Kernel	5.13.0-30
Nvidia drivers	510.47.03
CUDA	11.6
Python	3.8.10

Table 1: Used versions of operating-system, Python, Nvidia drivers and CUDA.

Name	Version	Use
Numba	0.53.1	GPU code generation
CuPy	9.2.0	access to pre-written GPU-functions
scikit-image	0.18.1	advanced image/matrix functions
tqdm	*4.61.1*	*progress bars*
tabulate	*0.8.9*	*improved class descriptions*

Table 2: Overview of utilized Python-packages used in the class responsible for data-generation. Italicized entries are not directly used in the simulation and are only for ease-of-use purposes.

3.2 Speed Comparison Between Sequential and Parallel Implementation

As expected, the parallel implementation of the SSM significantly outperforms the sequential implementation. Although more work has been done to ensure the parallel implementation is optimized appropriately, by large this difference in performance is due to the way the lattice is updated. The parallel implementation's ability to update $(L \times L)/8$ lattice sites at once performs equally well to the sequential implementation for low choices of L. For higher L the ability to update parts of the lattice at once allows for significantly lower update times for the whole lattice.

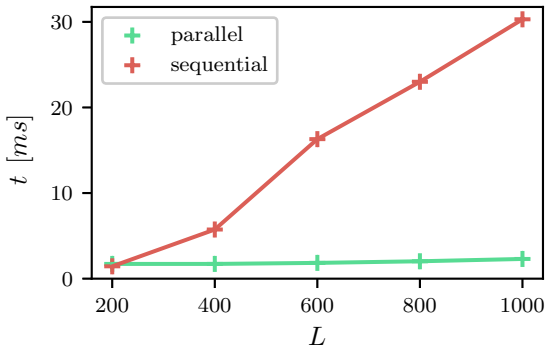

Figure 17: Average time needed to update whole lattice of a size L.

Surprisingly, the update-time for the sequential implementation rises almost linearly with the system length L. Since each lattice-update requires $L \times L$ local updates steps, the total update-time would be expected to rise with L^2. However, due to parallel implementation's significantly better performance no further investigation was conducted into this abnormal behavior of the sequential implementation.
As already mentioned in section 2.3, the parallel method of updating the SSM is used in all conducted simulations.

3.3 Differences between Sequential and Parallel Implementation

To compare some results between sequential and parallel implementation, the uninterrupted spread of a single species was simulated. This means that one cell in the middle of the lattice was populated with a species able to invade the surrounding empty lattice sites. Due to a large enough lattice, no interactions with the boundaries occurred in the simulated time-frame. The results (as measured by area and boundary length) are presented in figure (18). The simulations utilizing the sequential selection scheme grew marginally faster. As the boundary length at $t-1$ directly influences the possible area gained by time-step t, both A and B must be considered in conjunction. Additionally, the standard deviation of both area and boundary length are increased for the sequential selection scheme.

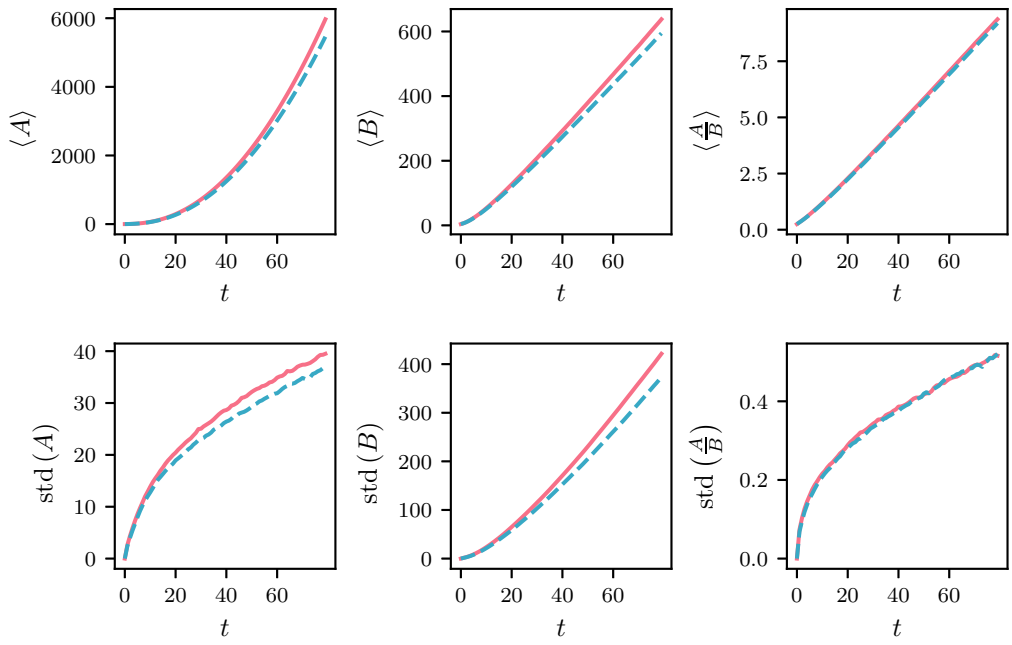

Figure 18: Area A (sum of all occupied cells), boundary length B (number all occupied/unoccupied pairs) and the ratio $\frac{A}{B}$ for the growth of single species in an empty lattice. Based on 10000 simulations. In each plot the blue line represents data from based on the parallel selection method, whereas the pink line corresponds to the random sequential generation method.

While these deviations in area and boundary length appear minor, they could result in differences between the sequential and parallel implementation. To illustrate how the choice of selection scheme is affecting the probability of ending up in certain states, an example is show below. While this example is obviously a large simplification from the real model, it could be especially relevant in stochastic patch creation. If one considers the interaction between two species, it is impossible to form patches when both species touch another in a complete straight boundary. Only when the contact-boundary between the species isn't perfect, stochastic patch creation can occur. This is illustrated in figure (18). This is obviously a hypothetical example, as the update-rules make it unlikely that a species expands in a straight line to begin with. However, it highlights how inhomogeneous spatial spread of a species (exemplified by the following tower building example) can be beneficial to stochastic patch creation.

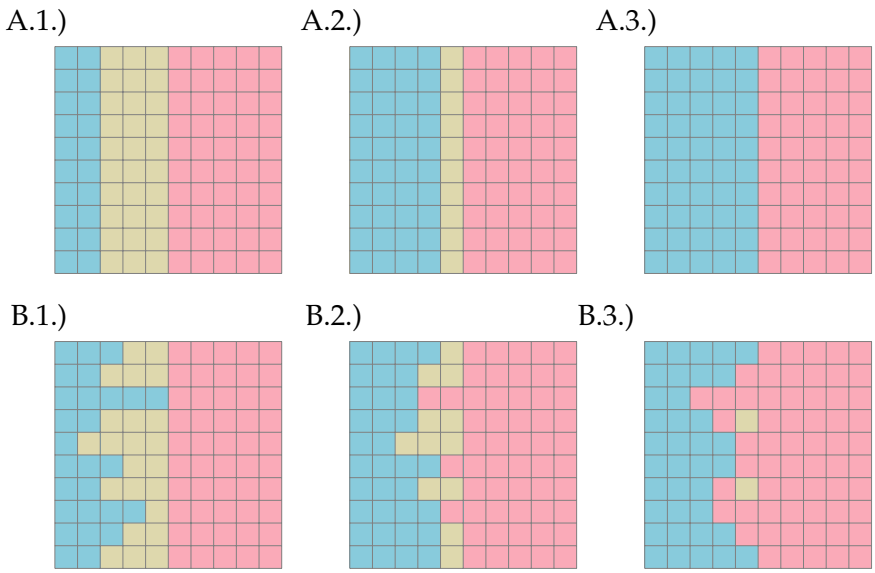

Figure 19: Illustration of how inhomogeneous spread can aid stochastic patch creation.
(A) Unlikely example of completely homogeneous expansion.
(B) Inhomogeneous spread leads to the creation of two isolated patches.

Example: Tower Building

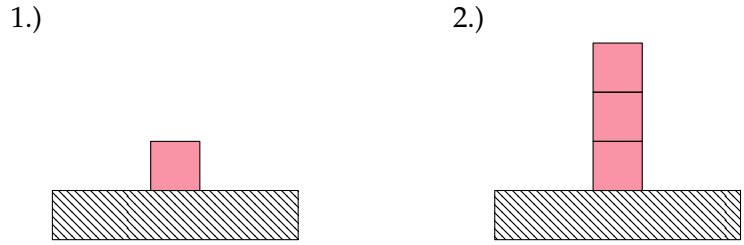

Figure 20: Illustration of the tower building example.

Assuming an initial state as displayed in figure (20.1), one wants to calculate the probability of ending up in the state displayed in figure (20.2), given the following interaction rules:
The red species cannot take over any of the hatched squares, but it can expand into the surrounding white area. For a detailed discussion, one could consider three species (red, hatched, and white). Here only the simpler yet equivalent case of one (red) species spreading is considered.
For the sequential selection calculating the probability is trivial. At every time-step the red species can expand in any direction it has an empty space adjacent. However, only one direction has the desired effect. This results in the probability

$$p(n) = \prod_{i=2}^{i=n} \frac{1}{2n-1} \tag{19}$$

of building a tower of height n. For the case of $n = 3$ this leads to $p(3) = 0.0\overline{6}$.
For the parallel selection scheme, calculation is more involved. This time it is necessary to keep track of the currently active 2×2 blocks as well as the height of the tower. The transition probabilities between the individual states are denoted in figure (21).

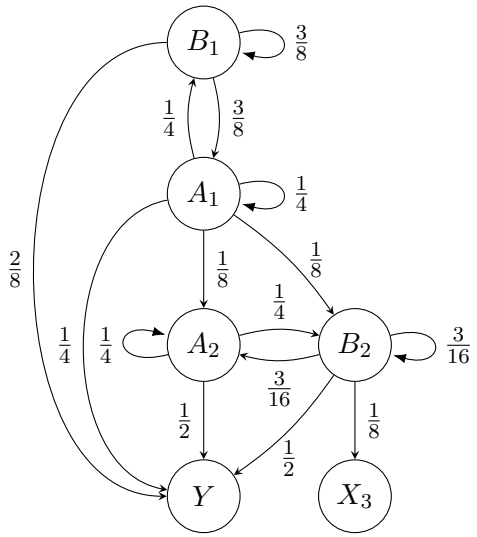

Figure 21: Transition network for the tower building example. The letters (A,B) indicate which subsection of the lattice is active and the subscript lists the current height of the tower. X_3 is the state corresponding to desired height of 3, regardless of which subsection of the lattice is active. Y indicates any other state.

This results in a transition matrix of

$$P = \begin{array}{c} \begin{matrix} B_1 & A_1 & A_2 & B_2 & X_3 \end{matrix} \\ \begin{pmatrix} 3/8 & 3/8 & 0 & 0 & 0 \\ 1/4 & 1/4 & 1/8 & 1/8 & 0 \\ 0 & 1/4 & 0 & 1/4 & 0 \\ 0 & 0 & 3/16 & 3/16 & 1/8 \\ 0 & 0 & 0 & 0 & 1 \end{pmatrix} \end{array} \begin{matrix} B_1 \\ A_1 \\ A_2 \\ B_2 \\ X_3 \end{matrix} \tag{20}$$

Resulting in a probability of $p_{abs} \approx 0.02722$ of reaching the desired state at any point. In this example, the sequential selection scheme is more than twice as likely to end up at a height of 3. This means that the parallel selection scheme has a higher chance of developing these protruding structures, resulting in more inhomogeneous species growth. As illustrated in figure (19), this could affect patch creation, and in turn the diversity of the system.

4 Results & Discussion

As the results in the following sections are loosely connected with each other, a quick summary is given to highlight how individual sections complement and build off each other. The appropriate section numbers are placed in brackets at the end of each description.

After the discussion of some initial problems in the generation of stable high diversity states (4.1), a more reliable method of generating these states is introduced (4.2). Since this method relies on introducing multiple species at once to build diversity, the average diversity and number of patches are compared between two different introduction rates n_{intro} (4.3). Additionally, the distribution of species (4.4) and patch sizes (4.5) is discussed. This is followed by a closer look at the distribution of time between the static states. To gain a better understanding of what caused the problems discussed in section 4.1, smaller system sizes are investigated (4.7) and the behaviour between SSM-simulations of different sizes are compared (4.8). Afterwards, the effects of inhomogeneous ecosystems are investigated. The unmodified model characterized in the preceding sections serves as a reference point. To start off, the effect of removed lattice sites is described (4.9). To see how adjacent systems interact with each other, a split ecosystem is introduced in section (4.10). There the lattice is split in the middle and each sub-lattice receives a different interaction network. Special attention is paid to the area where the two sub-lattices interact. Building on these results, a model with random interaction-network assignment is investigated (4.11). Finally, the effect of cyclic interactions is discussed and compared to previous research (4.12).

L	γ_{min}	γ_{max}	n_{sim}	n^{build}	n^{measure}
200	0.01	0.07	8	5000	5000
252	0.02	0.1	9	4000	4000
300	0.01	0.1	10	4000	4000
352	0.02	0.1	9	4000	4000
400	0.02	0.1	13	5000	5000
600	0.04	0.12	9	4000	4000
800	0.07	0.11	5	2500	2500
1000	0.08	0.1	3	2500	2500

Table 3: Simulations of the unmodified SSM. Lowest and highest choice of γ, the number of simulations n_{sim} and the number of static states in building-phase n^{build} and measuring-phase n^{measure}.

While only systems of size 400×400 are explicitly discussed in the following sections, the results apply to all sufficiently large system. Results for other system sizes are shown in the appendix.

4.1 Generation of Initial Conditions

In the initial simulations i.e. [23] initial conditions were provided through two separate mechanisms. The main implementation introduced 100 species in the first 100 time-steps. These starting conditions should show a fluctuating diversity at first and settle into a high-diversity state after the initial dynamics are concluded. However, this method was only used in simulations with $\alpha > 0$. Quasi-static simulations were initiated from previously obtained high-diversity states with similar γ-values. The intent behind this change in initial conditions was to speed up simulations.

Since there was no previous data available to serve as initial conditions, the method of generating initial conditions for the $\alpha > 0$ case from [1] were attempted in the case of $\alpha = 0$. However, despite multiple attempts, the simulation failed to produce stable high-diversity states in the majority of simulations. To rule out that this change in the systems behavior was due to the parallel-update rule, the sequential update rule was implemented. In either case, the introduction of 100 species into a grid of size 200×200 very rarely resulted in the creation of high diversity states, regardless of γ.

With the method of updating the system ruled out as the cause for the change in behavior, the only remaining explanation is that the noise added to the system by the introduction of new species in the case of $\alpha > 0$ allowed the creation of high-diversity states, and that the structure built in this process was stable enough to allow the diversity to persist in the quasi-static case.

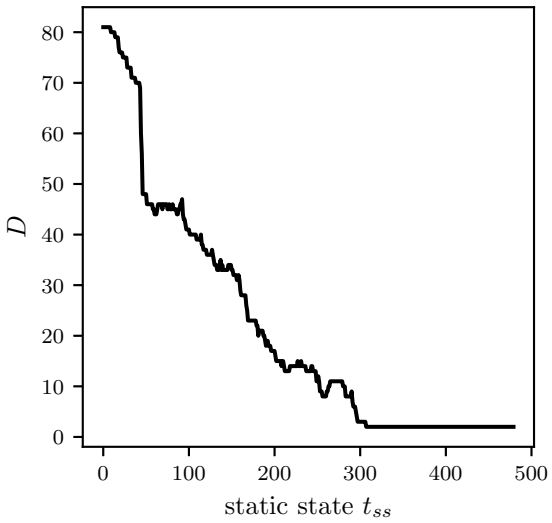

Figure 22: Diversity as a function of static state in a system of size 200×200. Out of 100 initially introduced species only 80 are still alive when system reaches the first static state a $t_{ss} = 0$. The system diversity continues to decrease until the $D = 1$ state is reached, approximately 300 static states later.

In order to investigate further, different combinations of starting species and lattice sizes were attempted. Keeping the lattice size the same while increasing the number of starting species slightly increased the time

spent in a high diversity state. However, the system still had a tendency to collapse and would do so in most attempts. Another set of simulations was conducted with both system size as well as the number of starting species increased. Systems with $L = 300$ and a starting diversity of 1000 showed a noticeably better chance of settling into a high diversity state. Similar odds of settling into a high diversity state were found for all systems with $L \geq 252$ and the number of starting species up-scaled appropriately from the choices in [23]. As these simulations were only attempts of finding a sufficiently reliable way of generating high diversity states, no statistics were kept about the chance of generating a stable high diversity state. However, even with refined parameters this method of generation was deemed unreliable in the generation of high-diversity states.

Parts of the behaviour discussed in this section could be due to the system being not big enough to build stable diversity in the quasi-static case. The following section introduces a significantly more reliable method of building high diversity states. However, even this method fails do deliver consistent results for low enough system-sizes, as will be discussed in section 4.7.

4.2 Building Stable High Diversity States

As explained in the previous section, the methods used for the generation of high-diversity states from prior papers are not sufficient in the generation of stable, high-diversity states in quasi-static simulations. However, with a simple modification high-diversity states can be achieved consistently, even with $\alpha = 0$. In [1] and [25] it is already discussed that the introduction of more than one species every time the system reaches a static state causes the low diversity state to vanish. As such, static-state introduction rates of $n_{intro} \geq 2$ can be used to force the system into high-diversity state.

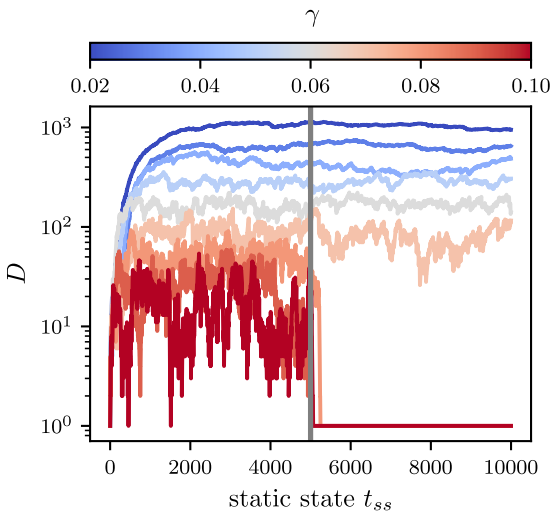

Figure 23: Diversity time-series for various of γ with $n_{intro} = 2$ for $t_{ss} < 5000$ and $n_{intro} = 1$ for $t_{ss} \geq 5000$.

Specifically, the system is initiated completely empty, but with a static-state introduction rate of $n_{intro} \geq 2$. (In some figures n_{intro} will be shortened further to n.) Other than that, no changes are made, and the simulation starts. Depending on system-size L and interaction-probability γ, the system's diversity should saturate in a high-diversity state after some time. At this point the static state introduction rate is reduced back to 1. This makes it possible for the system to collapse to its low-diversity state. Figure (23) shows the diversity D during this process. For $t_{ss} < 5000$ (left of the grey line) two species are introduced at every static state, afterwards only one.

Some initial experiments were carried out with higher values of n_{intro}. The behaviour for all values $n_{intro} \geq 2$ was similar. Higher values resulted in slightly faster initial diversity growth. If the introduction rate was significantly increased (i.e. $n_{intro} \geq 10$), it was possible to achieve diversities noticeably higher than the ones expected based on figure (24), especially for high γ. However, if the introduction rate was reduced back to 1, diversity fell to the values displayed in figure (24). As a result, it seems unlikely that there is another set of meta-stable states with diversities above the ones that have so far been described as the high-diversity states.

Unless specified explicitly, this method of generating stable high diversity states is used in all experiments. All measurements were taken far enough after the initial buildup in diversity or the change in n_{intro} to ensure that transitional effects are recorded. The initial phase with $n_{intro} = 2$ will be referred to as the *building phase* and following phase with $n_{intro} = 1$ as the *measuring phase*.

4.3 Average Diversity & Number of Patches for $n_{intro} = 2$ and $n_{intro} = 1$

Additionally, to providing a reliable way of generating stable, high-diversity states, the method introduced in the previous section also provides a new set of data. While initially discussed in [1], systems with $n_{intro} = 2$ and $n_{intro} = 1$ have not been compared in full detail so far.

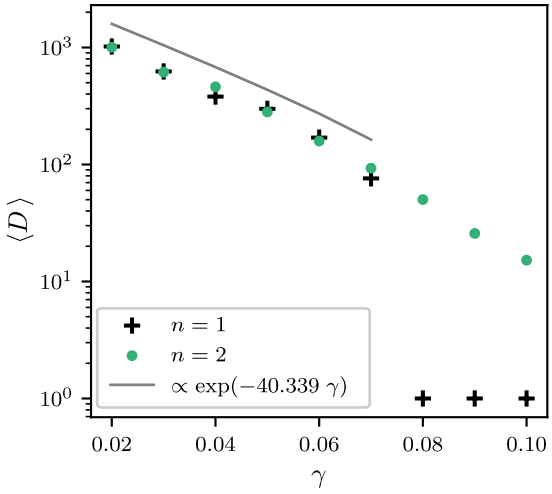

Figure 24: Average Diversity for a system of size 400×400 for various values of γ. The building phase is indicated by $n = 2$ and the measuring phase by $n = 1$

Figure (24) displays the average diversity for a system of size 400×400 as a function of γ. While the $n_{intro} = 1$ case collapses to the low diversity state for $\gamma \geq 0.07$, the $n_{intro} = 2$ version shows no notable change. Both the collapse for $n_{intro} = 1$ and the lack thereof for $n_{intro} = 2$ are expected, based on the research introduced in the previous sections. In further analysis the critical values of γ is assumed to be between 0.07 and 0.08.

For all simulated values of n_{intro} the diversity grows exponentially with reducing values of γ. Based on figure (24) alone, one could assume that the systems show no drastic change in structure for $\gamma > \gamma_c$ in the building phase.

The average number patches, as displayed in figure (25), clearly shows a change in behavior for supercritical values of γ. Both $n_{intro} = 2$ and $n_{intro} = 1$ are almost constant for $\gamma < \gamma_c$. As expected, the number of patches drops to 1 for $n_{intro} = 1$ and $\gamma > \gamma_c$. Unlike in the case of average diversity, the average number of patches shows different behavior for $\gamma > \gamma_c$. Instead of staying at a value between 7000 and 8000, it drops with increasing γ. A closer look at the time series of P shows that this drop in average is due to number of patches

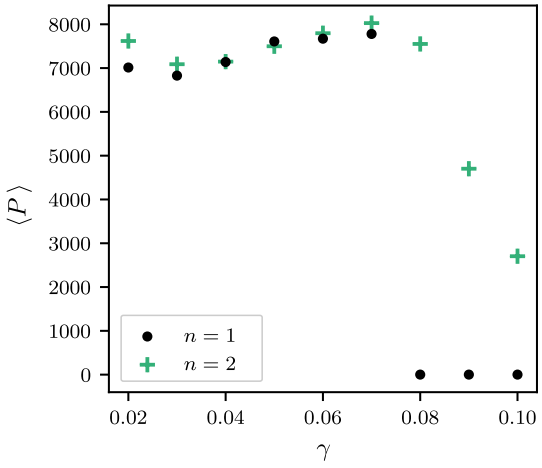

Figure 25: Average Number of Patches for a system of size 400×400 for various values of γ and two consecutive choices of n.

fluctuating between high values (> 7000) and low values (< 200). As displayed in figure (26), for $\gamma > \gamma_c$ can even lead to more patches for $n_{intro} = 2$.

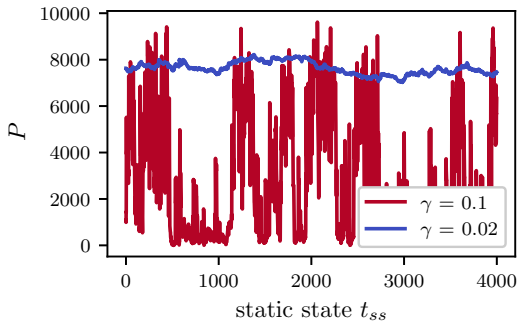

Figure 26: Number of patches in a system of size 400×400 for $\gamma = 0.1$ and $\gamma = 0.02$ in the case of $n_{intro} = 2$.

This is not necessarily surprising, as the $D = 1$ state is not absorbing with $n_{intro} = 2$. However, it is likely that the system is unstable. Therefore, one would expect the system to collapse to a state of low diversity and recover again after some time. Even the heightened number of patches in the $n_{intro} = 2$ case could be explained when cyclic patch creation is considered. The collapse of the system for $\gamma > \gamma_c$ clears large areas of the lattice and a following cyclic interaction can therefore create more patches. An example of this is shown in figure (27). Additionally to showing a drastic increase in the number of patches, the figure also highlights how short lived structures are for $\gamma > \gamma_c$. As seen in figure (28, in the sub-critical case, usually only minor differences are visible. Whereas in the super-critical case, the entire lattice changes multiple times with the introduction of a few species.

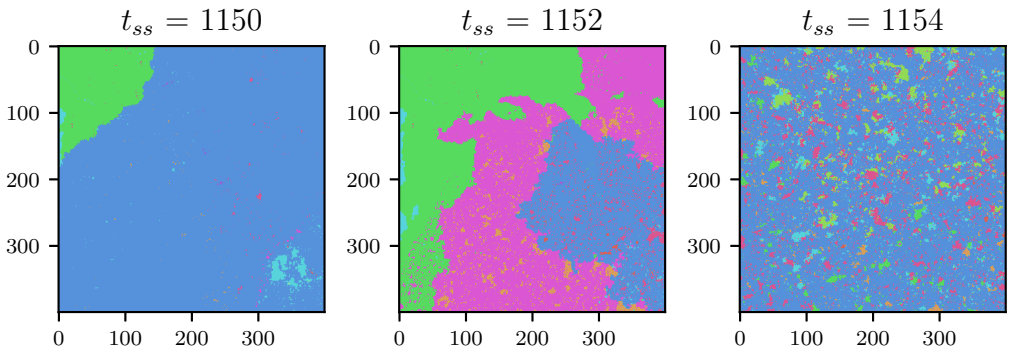

Figure 27: Development of patches in a system of size 400×400 with $\gamma = 0.1$ and $n_{intro} = 2$. Over the course of 4 static states the diversity drops from 16 to 11, the number of patches increases significantly from 792 to 6852.

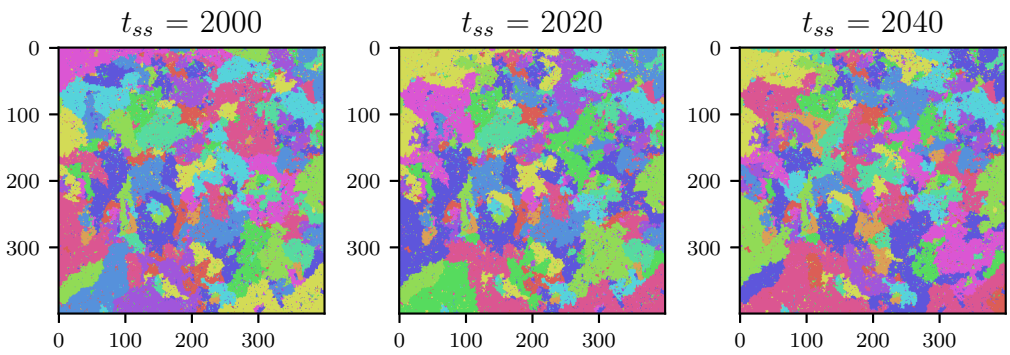

Figure 28: Development of a system of size 400×400 with $\gamma = 0.02$ and $n_{intro} = 2$. Over the course of 40 static states, the diversity drops from 963 to 959, and the number of patches increases from 7374 to 7600. Even though a 10-times longer timescale is displayed, the states are visually more similar to each other than in comparison to the supercritical case displayed in figure (27).

4.4 Species Size Distribution

To gain further insight into the structure of generated states, it is helpful to look at more metrics than just diversity and the number of patches. An obvious choice is the distribution of lattice sites belonging to each species. This defines the species size s for a species with index i

$$s(i) = \sum_{x,y=1,\dots,L} \mathbb{1}\{\text{ species at } (x,y) = i\} \tag{21}$$

Where $\mathbb{1}$ is the indicator function following the simplified definition $\mathbb{1}\{x\} = 1$, if condition x is fulfilled and 0 otherwise. Like the discussion of average diversity and patch number in the previous section, the data generated during the $n_{intro} = 2$ phase, could give some insight into the structure of states that would collapse with lower introduction rates. Once again, equal values of γ show similar behavior for $n_{intro} = 2$ and $n_{intro} = 1$. This is with the obvious distinction that there are more non-collapsing values of γ for the introduction-rate of 2. The complementary cumulative distribution functions for the species sizes, ccdf(s), are displayed in figure (29.A).

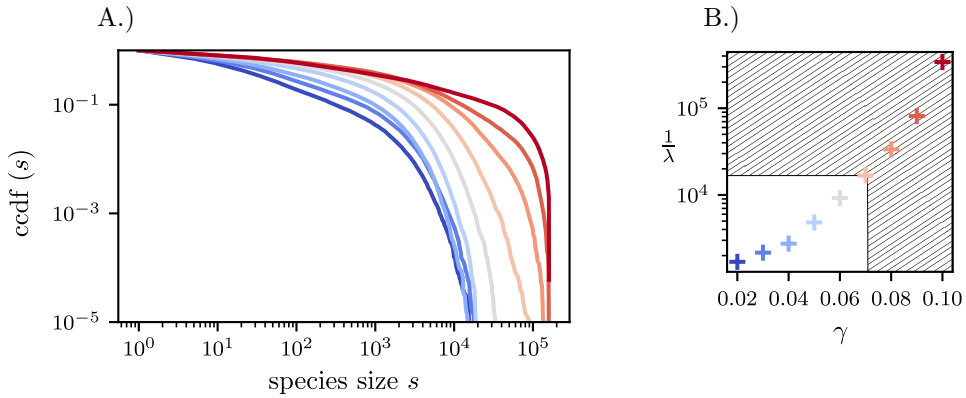

Figure 29: A.) ccdf of species sizes for a system with $L = 400$ during its diversity building phase. B.) $1/\lambda$ for the fitted powerlaw (equation 22) is shown to give a rough estimate of where the truncation is noticeable.. The area marked by the hatch-pattern indicates all γ and approximated λ that collapsed when the introduction rate was reduced to 1.

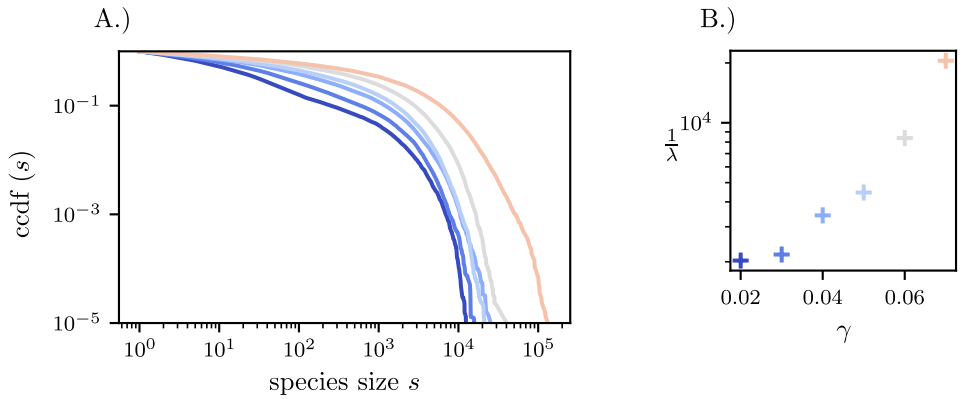

Figure 30: A.) ccdf of species sizes for a system with $L = 400$ during its measurement phase. B.) $1/\lambda$ for the fitted powerlaw (equation 22) is shown to give a rough estimate of where the truncation is noticeable.

As already noted in previous research [23], species with high populations occur less frequently, seemingly following power-law with a truncation. The data displayed in figure (29) shows that high values of γ correspond with the truncation occurring at higher values for both building as well as the measuring-phase.

To analyze the truncation further, a discrete, exponentially-truncated power-law-distribution

$$p(x) = Cx^{-\alpha}e^{-\lambda x} \tag{22}$$

was fitted to measured species-sizes using methods from [30]. In equation (22), C is chosen to ensure that $\sum_{x=x_{\min}}^{\infty} p(x) = 1$. Two representative examples are shown in figure (31). Both visually fit well with the data and are statistically preferable to other tested distributions (exponential, power-law, ...).

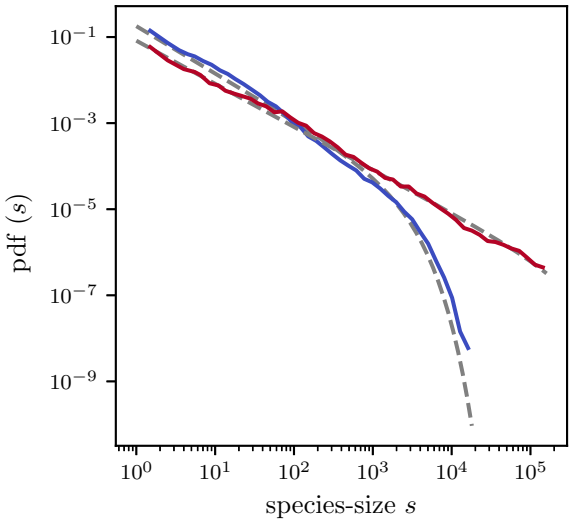

Figure 31: 2 Examples of the truncated power-law fit for the cases $\gamma = 0.02$ and $\gamma = 0.1$ in a system of size 400×400.

4.5 Patch Size Distribution

Like the species-size distribution discussed in the previous section, the distribution of patch-sizes can be quantified in a comparable way. Here, a patch is defined as a connected cluster of the same species, with adjacency on the lattice defined through von-Neumann neighborhoods.

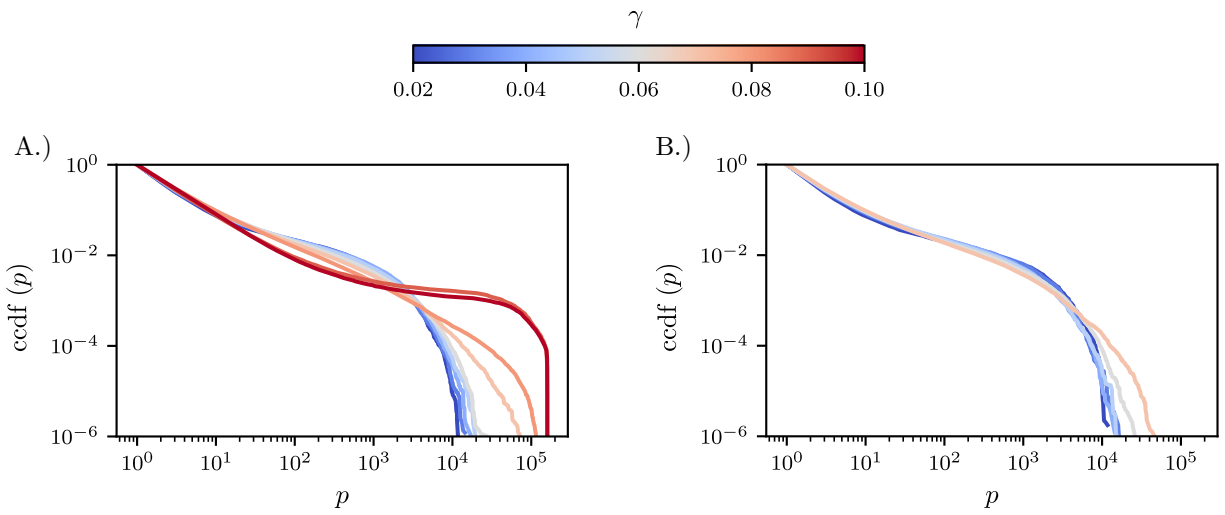

Figure 32: ccdf for patch sizes in a system of size 400×400. (A) depicts the building phase and (B) the measurement phase.

Figure (32) shows how the patch-size ccdf undergoes a noticeable change as γ increases. All values of γ far below the transition point show similar behavior and have a maximum patch size of approximately 2×10^4. Interaction probabilities closer to the presumed transition point of $\gamma_c \approx 0.75$ show an increase in the observed maximum patch size. Even higher γ-values finally let the maximum patch size get close to its maximal value of 1.6×10^5.
Given the differences in the patch size distribution between $\gamma \leq 0.06$ and $\gamma > 0.06$, the previously assumed critical point of 0.075 seems to be too high. After-all, one would expect the patch-size distribution and the diversity to change their behavior at the same value of γ. Following this assumption, the observed stability in the simulation with $\gamma = 0.07$ could only be the result of a too short simulation window. However, this behavior is less noticeable in for $n_{intro} = 1$ in figure (32.B), warranting further investigation to reach a conclusion.

4.6 Distribution of Time between Static States

To determine how many lattice updates are between static states and at what rate new species are introduced into the system, the time between static states has been recorded for most simulations. Once again, a system of size 400×400 has been chosen as an example and the results are displayed in figure (33). As both introduction rates resulted in almost identical results, only the $n_{intro} = 2$ case is plotted. The probability of the system dynamics stopping soon after the introduction of a new species is similar for all values of γ. This is likely due to the new species landing in one of the many small patches present for both $\gamma < \gamma_c$ and $\gamma > \gamma_c$, taking over the patch but not being able to invade the surrounding area. Both the sub-critical as well as super-critical values of γ seem to have a characteristic time for system dynamics.

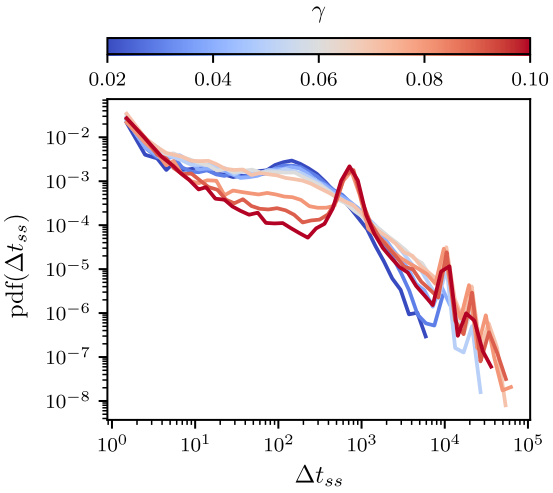

Figure 33: Empirical probability density function for the time between static states Δt_{ss} for a system of size 400×400. Since n_{intro} is set to 2, the $D = 1$ state is not absorbing and it is possible to gain an intuition into the behaviour of systems with high γ. Kernel density estimation was used to simplify the plot. However, this causes narrow peaks to be smoothed out slightly.

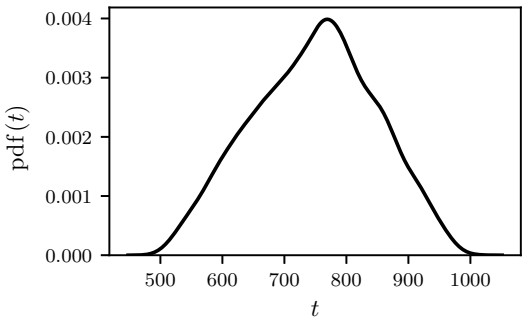

Figure 34: Empirical probability density function for the time needed to spread to all parts of a lattice of size 400×400. The data-set consists of 10000 simulations with randomized initial conditions.

In the sub-critical case, the distinction is less pronounced, yet the probability density function of Δt_{ss} is increased around 150 updates. The behaviour in the supercritical case is more noticeable, showing a peak in probability for $\Delta t_{ss} \approx 800$.

This effect might be best described by considering the super-critical case first. As already visible in the example displayed in figure (27), states in systems

with $\gamma > \gamma_c$ and n_{intro} tend to have patches that span a large part of the entire system. Since the size of a patch determines how like likely a new species will land in it, these large patches are also the most likely candidate for the placement of a new species. From there, the new species will spread over the entire area of the largest patch, which will take roughly as long as it would take to fill the entire lattice. The time-distribution for filling an entire 400×400 lattice is displayed in figure (34). For $\gamma < \gamma_c$ the system forms more complex structures and the time to fill the initial patch is therefore less consistent. However, it could explain the slight increase in the probability density function displayed in figure (33).

While the spikes occurring for values of $\Delta t_{ss} = 10^4$ and multiples thereof seem significant at first, they are only artifacts of the acceleration method used for cyclic interactions, as described in section 2.4. If the dynamics in the system take longer to complete than $\Delta t_{ss} = 10^4$ lattice updates, one active species loses all of its interactions temporarily. This has a chance to stop cyclic interactions and the system settles into a stationary state soon afterwards. If the chosen species did not belong to an active cycle, or there were multiple cycles occurring simultaneously, the process repeats for multiples of $\Delta t_{ss} = 10^4$. As such, all peaks in the probability density function for $\Delta t_{ss} \geq 10^4$ can be explained through the acceleration of cyclic interactions.

4.7 Lower Limit of Stable System Sizes

As already mentioned in section 4.1, a system size of 200×200 caused significant difficulties in the generation of stable high diversity states. This was based on preliminary tests performed using the initial condition method from [23]. Therefore, it is of interest to see if the method for generating high diversity states introduced in section 4.1, shows similar problems for low systems sizes. For the, up until now, discussed system size of 400×400, the method produced (stable) high diversity states with very high reliability.

To further investigate the behavior of the system for lower system sizes, systems with $L \in \{200, 252, 300, 352\}$ were simulated for a range of γ-values. The results are displayed in figure (35). The cases with $L \in \{252, 300, 352\}$ show similar behavior to the $L = 400$ case, displayed in figure (23). For $L = 200$ the diversity time-series appear inconsistent with all other tested systems and results from previous research. The diversity collapses for all but one value of γ. Additionally, the interaction probability

seems uncorrelated to the stability of the system, exemplified by system with $\gamma = 0.01$ (the lowest in the set of conducted experiments), collapsing significantly earlier than the system with $\gamma = 0.04$.

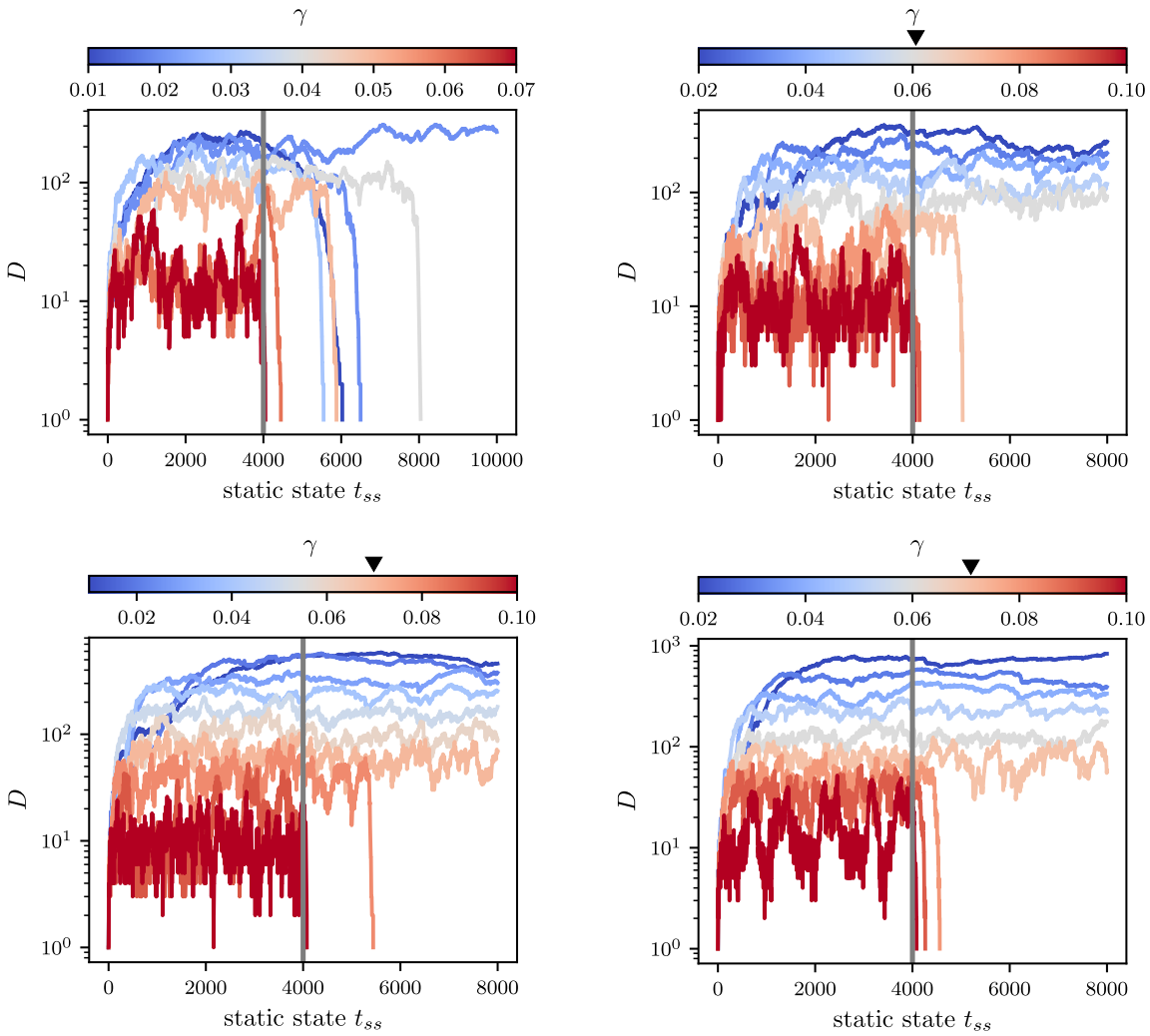

Figure 35: Diversity time-series for systems of size $L \in \{200, 252, 300, 352\}$ and various γ. The highest stable γ is indicated with a ▼ in the colorbar.

Since both methods for initial condition generation run into problems when simulating low system sizes, the system's instability might due to its size. In the [23] this effect could have been masked by the use of initial conditions from simulations with random species introduction.

On closer inspection of plots in figure (35), it is also visible that the simulations with the highest unstable γ remain in a state of high diversity for a longer time than they did in the case for $L = 400$. This effect is especially pronounced for $L = 252$ and $L = 300$. However, as this effect is also visible for larger systems-sizes, it presumably has more to do with how close the chosen γ is to γ_c. This gives further evidence that the collapse to diversity 1 in a finite time-frame might not be the best way to determine a systems stability.

4.8 Comparison of System Sizes

After discussing the lower end of stable system sizes in the previous section, the following section focuses on the SSM's behavior for all system-sizes. While the amount of available data was limited by the long simulation-time of individual systems, especially for large L and γ, a pattern is clearly visible.

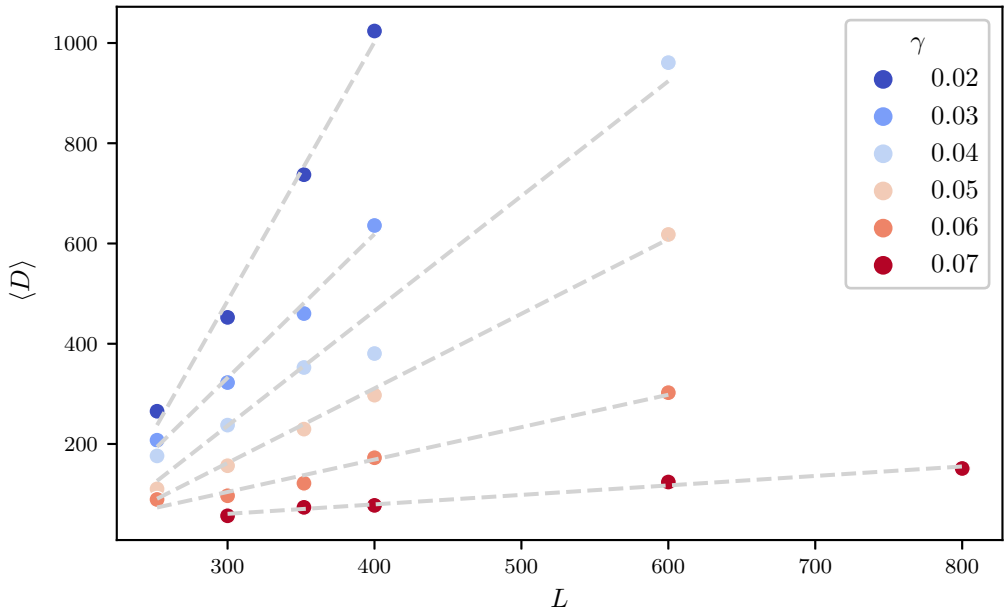

Figure 36: Average diversity in stable states with $n_{intro} = 1$ for a range of γ and L. Data-points are only included if a γ-values was available for multiple lengths L. Linear regression slopes are added to guide the eye and roughly quantify the behavior of $\langle D \rangle(\gamma, L)$. The slopes of this linear regression are displayed in figure (37).

Figure (36) shows how the average diversity changes as a function of system-size for different values of γ. For any given value of γ, the average appears to grow linearly with system length L. To highlight this and quantify how the slope changes for different values of γ, a linear regression has been applied to the data-points. Overall, higher values of γ result in lower slopes.

Figure (37) shows how the slope relates to γ for the acquired data. While the displayed points seemingly follow a exponential-function, one must be careful with further interpretation, as the noise in the initial data could be amplified by the linear regression. Furthermore, the number of available γ-values is still limited, despite the simulation speed improvement due to the parallel implementation.

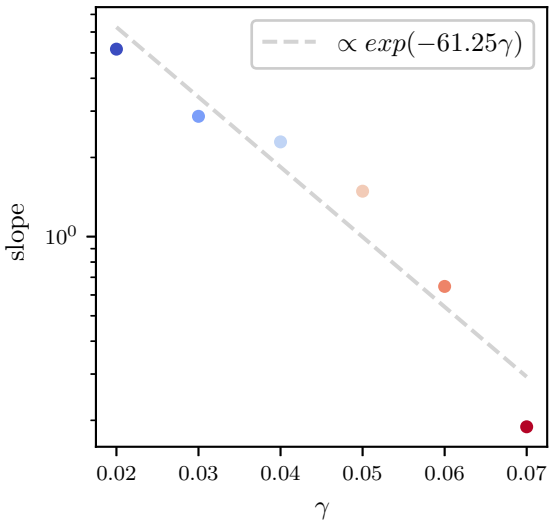

Figure 37: Slopes of linear regressions fitted to the data displayed in figure (36).

However, it is clear that the slope scales negatively with γ in the selected region of L. Negative values for the slope would imply that small systems have high diversity for high enough γ. These simulations were already discussed in [1] and show the exact opposite effect - diversity collapses to its minimum. As a result, negative slopes can be ruled out, leaving 0 as the obvious lower limit for slope.

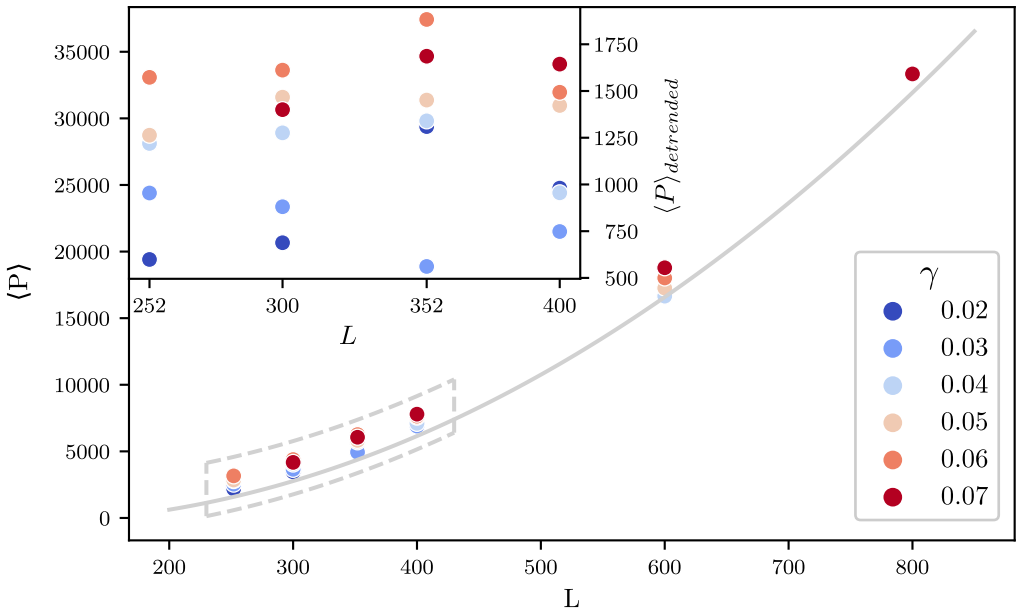

Figure 38: Average number of patches for various γ and L. To show how larger values of γ result in more patches on average, the trends in the data are removed with a second order polynomial (grey line), and sub-section is drawn in the inset (dashed gray rectangle).

As seen in figure 38, the average number of patches in stable, high diversity states grows super-linearly with system length L. To emphasize how higher γ led to a higher average number of patches, the data was de-trended with a second order polynomial and the result, for a selected range of L, is drawn in the inset. Comparing figure 36 and figure 38, it is obvious that a higher number of patches does not directly translate to a higher diversity, even in systems that remained stable for a significant period.

4.9 Ecosystems with Inactive Lattice Sites

To gain first insight into the behaviour of the SSM with altered spatial conditions, a set of simulations was conducted with randomly introduced, inoccupiable, lattice sites. This is equivalent to initializing the system with a completely neutral species. This species can't be invaded, does not invade other species and is not overwritten by the introduction of new species. The implemented code follows this interpretation, as it was more compatible with the existing code-base. For the discussion here, however, the terminology of removed/inactive lattice sites was chosen. In line with that, the model is referred to as the *inactive SSM*.

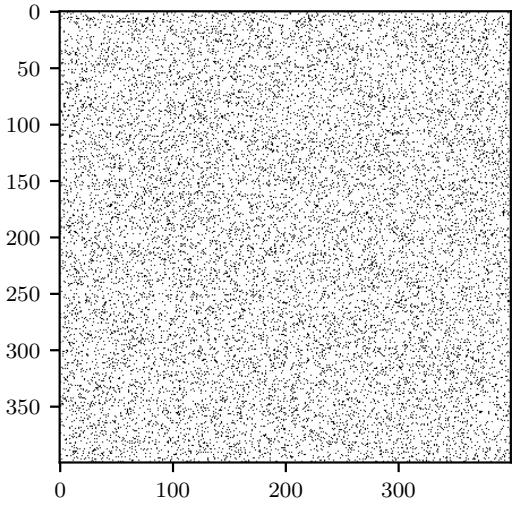

Figure 39: Initial state of a ecosystem with removed lattice sites. White lattice sites are inhabitable by all species, black sites are removed. The majority of all white lattice sites are connected.

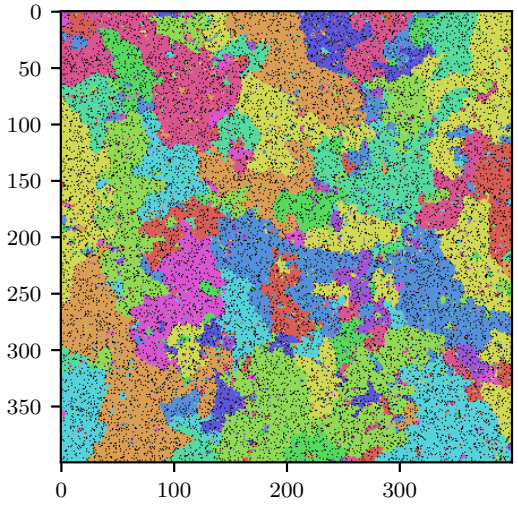

Figure 40: Example static-state for a SSM-ecosystem with 10% of lattice sites being completely inactive. The other system parameters are set to $L = 400$ and $\gamma = 0.02$. Inactive lattice sites are colored black.

A high probability of a lattice-site being removed, would make it more likely for clusters to be formed and could therefore result in the high-diversity phase being inaccessible due to the limited space available. In order to avoid this, the probability of a lattice site being removed is set to 10% for all simulations. However,removing lattice sites with a probability of 10% leads to an approximately 20% reduction in active neighbours.

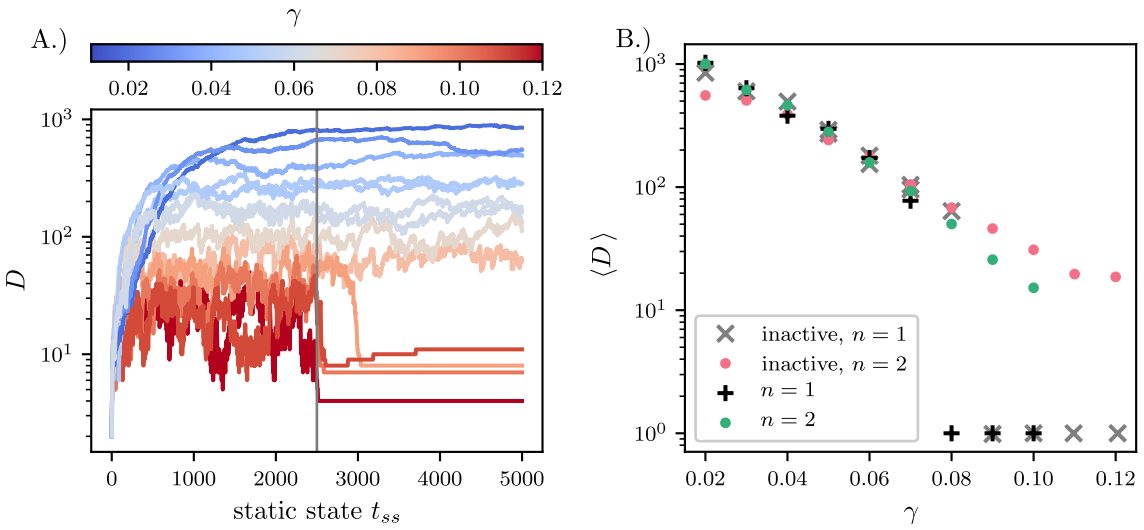

Figure 41: (A) Diversity time-series of an 400×400 ecosystem with 10% inactive lattice sites. (B) Average diversity for both the basic and the inactive-SSM. Only the largest, fully connected area is considered.

As seen in figure (41.A), the SSM with in-occupiable lattice sites shows similar behaviour to the basic version. One of the most noticeable differences is that the diversity never collapses to one. This is only due to very small patches of the lattice that are completely isolated from the surrounding system. This means every connected ecosystems still collapses to a state with diversity 1, if γ is high enough.

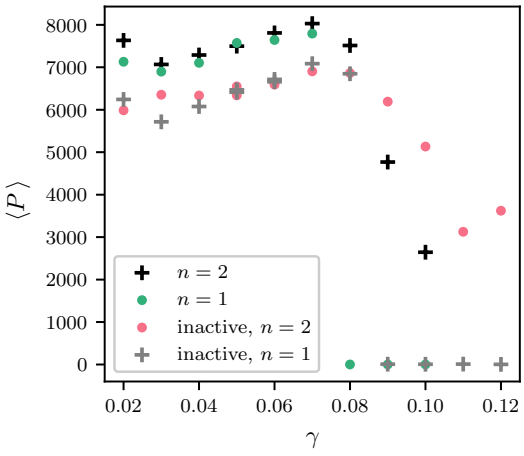

Figure 42: Average number of patches for both the basic and the inactive-SSM for building and measuring phase

Even the apparent increase in total diversity can be explained with disjoint subsystems changing their diversity. At $t_{ss} = 2500$ some of the separate patches are still empty and are counted as belonging to the same species. When a static state is reached and consequently a new species is introduced, it can land in one of these patches and take it over. Therefore, the diversity is going to rise over time as the empty subsystems get filled with different species.

The inactive SSM shows similar average diversity to the basic SSM for $\gamma \in [0.04, 0.07]$.

The lowest two γ seem to result in slightly less diversity in comparison. Higher γ show a marginally higher diversity and collapse later. Figure (42) shows that the number of patches for sub-critical γ is approximately 15% lower in the inactive-SSM.

4.10 Split Ecosystems

Another possible modification of the SSM is to increase the number of interaction-networks in the system, allowing for the modeling of ecosystems with inhomogeneous conditions. In this thesis, only spatial inhomogeneity is discussed. However, switching between interaction networks based on time also would be possible with the implemented code and could be used to model seasonal changes.

For the discussed spatial inhomogeneity, every lattice site (x,y) is assigned to one of two interaction-networks. This choice of interaction-networks will be referred to as the *condition* of the lattice site (x,y). Various ecological interpretations for this are possible: changes in the soil composition or different sun exposure (i.e. on a rock partially covered from direct sunlight). The best fitting interpretation obviously depends on how lattice conditions are chosen.

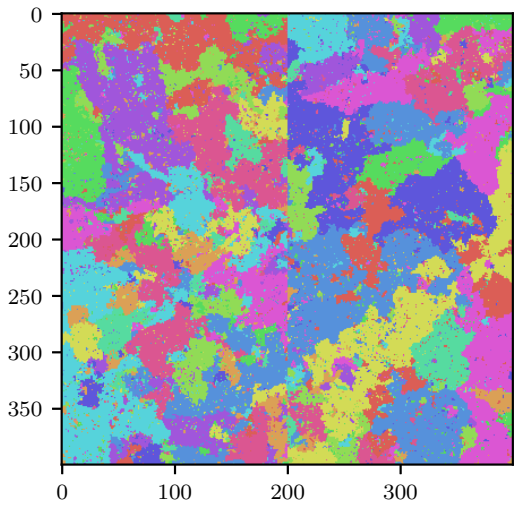

Figure 43: Example static-state of a split-SSM-ecosystem of size 400×400 and $\gamma = 0.05$. The boundary between the two areas with separate interaction networks is still visible at $x = 200$.

For the first example, the lattice has been split into two halves and each half has been assigned an interaction network. This is done to model the interaction between two adjacent SSM-ecosystems. As such, it could be interpreted as an ecosystem at the boundary between forest and open fields or as lichen growing on a rock partially covered from direct sunlight. To differentiate between the basic SSM and the model introduced above, this model will be referred to as the *split-SSM* and an example state is plotted in figure (43). The boundary remains visible despite the visual noise created by the individual patches. The boundary between the two halves is of special interest, as it could show so-called

edge effects - an either positive or negative change in local diversity caused by the change of environment. These effects are recorded in many empirical studies on the interaction of ecosystems and are of special interest in theoretical ecology [2]. The following paragraphs will show that split-SSM shows a positive edge effect at the interaction boundary.

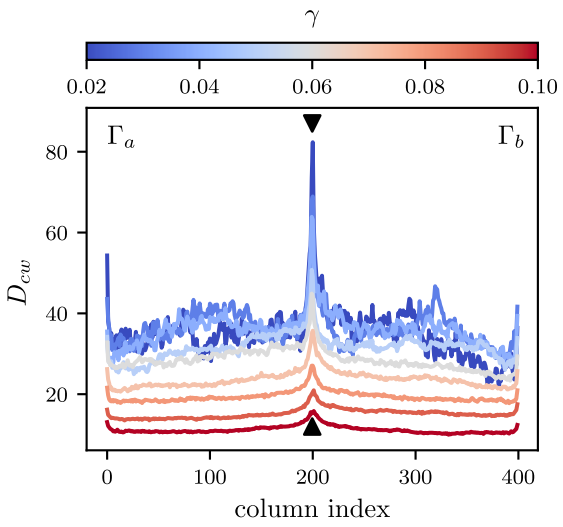

Figure 44: Column-wise diversity for various γ in a system of size 400×400. Only non-collapsing static states generated with $n_{\text{intro}} = 1$ are considered.

As seen in figure (44), the column wise diversity (meaning the number of active species in each column of the lattice), is significantly increased around the boundary between the two regions. This effect is visible for all values of γ but drops off rapidly further away from the center. Additionally, the column-wise diversity is increased around the edges of the ecosystem (column index $= 0$ and L in the column-wise depiction). This is likely due to another edge-effect, this time between the system and its closed outer boundary.

Figure (45.A) shows that the diversity-collapse in the split-SSM occurs for higher values of γ, when compared to the unmodified SSM. Additionally, one ecosystems remains in the meta-stable high-diversity state longer than observed so far. While some unmodified systems displayed in figure (35) show partially similar behavior, the split-SSM with $\gamma = 0.11$ displayed in figure (45.A) remains in it's high diversity state roughly 4 times longer before it collapses. This increase in time to collapse could be attributed to introduction of the spatial condition.

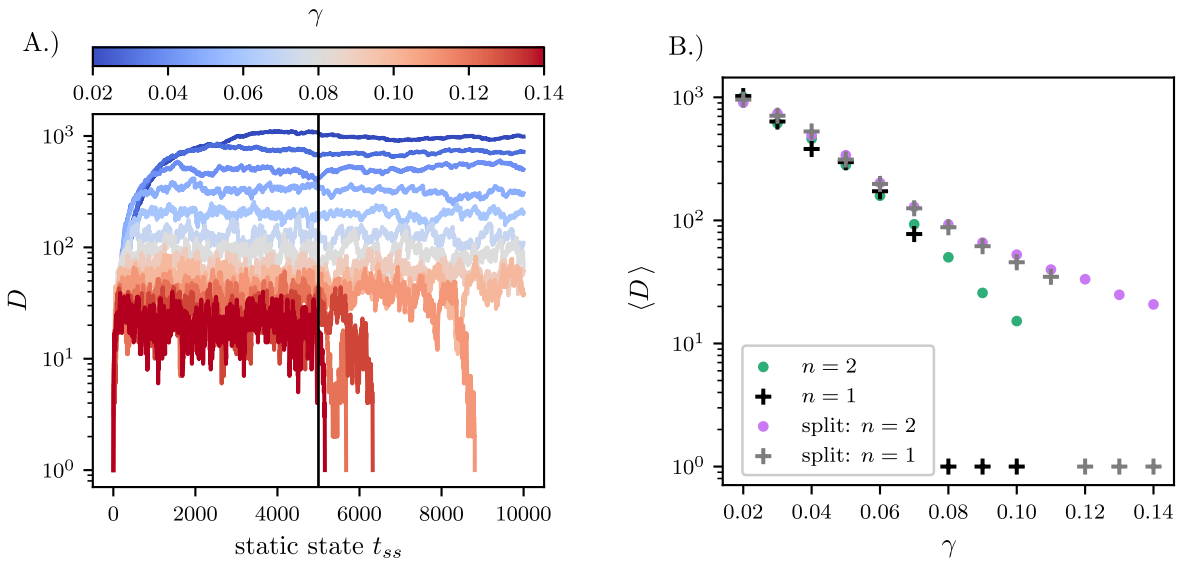

Figure 45: (A) Diversity time-series for a split SSM-ecosystem of size 400×400. (B) Average diversity for building and measurement-phases of the unmodified and the split-SSM. If a ecosystem collapses, it's average is assumed to be 0.

The comparison between the average diversities in the split-SSM and its unmodified counterpart, displayed in (45.B), show that in the split version $\langle D \rangle$ drops off slowly when γ is increased. Up until the point of collapse this is true for both the building and the measurement-phases.

Similar to figure (44), figure (46) shows an increase at the boundary of the two areas in the system. As already seen in figure (27), even unstable γ can lead to a large number of patches. As a result the column-wise number of patches for $\gamma = 0.08$ exceeds the column-wise number of patches for the case of $\gamma = 0.02$ in most places.

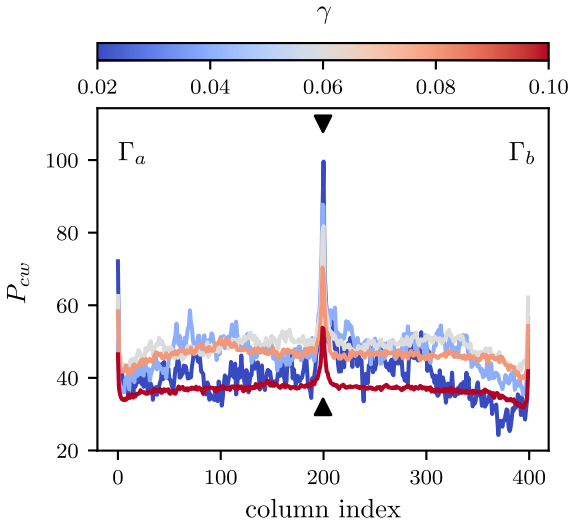

Figure 46: Column-wise number of patches for various γ in a system of size 400×400. Only non-collapsing static states generated with $n_{\text{intro}} = 1$ are considered. The number of displayed γ was reduced to minimize overlap.

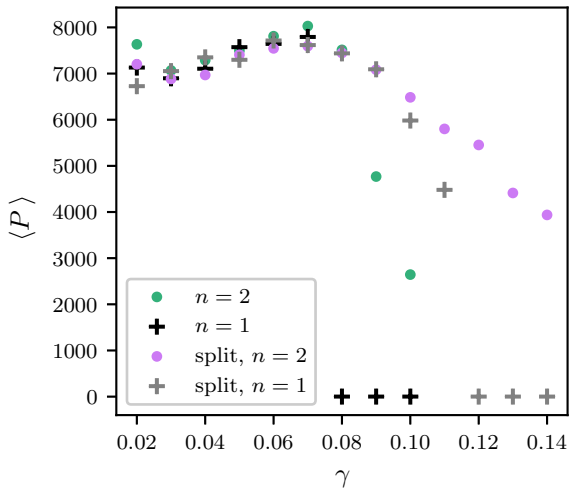

Figure 47: Average number of patches for building and measurement-phases of the unmodified and the split-SSM. Both with $L = 400$.

As seen in figure (47), the average number of patches for the unmodified and the split-SSM behave similar for $\gamma \leq 0.07$. In comparison, the average number of patches drops of slower for the split-SSM for $n_{intro} = 2$. A possible explanation for this is that the two spatial conditions reduce the chance that the entire lattice is overtaken by one species.

4.11 Random Condition Ecosystems

Another obvious choice of introducing spatial inhomogeneity into the SSM is to decide on the condition of a lattice-site randomly. As discussed in section 4.10, only systems with 2 conditions (referred to as condition A and condition B) are discussed in this thesis. This allows the introduction of a new parameter θ. When initializing the system, every lattice-site is assigned to condition A with probability θ and to condition B with probability $(1 - \theta)$. This modification of the sessile species model will be referred to as the *random-condition-SSM*.

As the random-condition-SSM introduces a percolation problem into the systems, the obtained results might be slightly harder to interpret. However, based on the results displayed in the previous section, it is simple to conjecture that the random assignment of conditions to system, and the resulting increase in boundary length between conditions, should affect the diversity in a positive way.

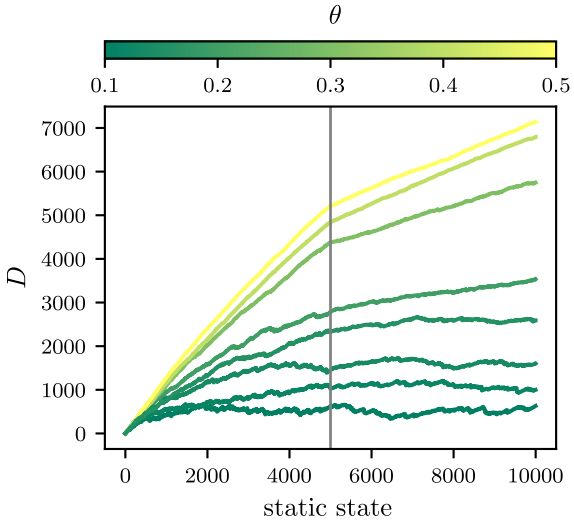

Figure 48: Diversity-time-series for 4 choices of θ in a system of size 400×400.

Before this possible change in diversity can be discussed, it is useful to have a closer look at the choice of θ. Figure (48) shows diversity-time-series for 8 choices of θ. Noticeably only low choices of θ saturate their growth in the simulation time. For all other θ, the diversity of the system increases throughout the simulation. It is obvious this increase in diversity has to stop when the system size is reached. While it would be interesting to see at what value the diversity saturates, due to the (presumably) very long simulation time needed, these experiments were not conducted. Out of all values of θ that finished growing in diversity during the allotted time, $\theta = 0.1$ was chosen as it allows for easier comparison to the inactive SSM in section 4.9.

Like other modifications of the SSM, the random-condition SSM produces visibly different states than the basic version or its other modifications. Figure (49) displays an example static state in a simulation with $\theta = 0.1$ and $\gamma = 0.1$. The randomly assigned conditions result in static states that look even more fragmented than in the unmodified case. The diversity time-series of the simulated random-condition SSM show significantly improved stability in comparison to the basic model. This is displayed in figure (50.B). Even the highest value of $\gamma = 0.2$ does not collapse to a state with diversity 1. While $\gamma = 0.2$ clearly shows large fluctuations in diversity, the structure of the lattice always allows some species to survive.

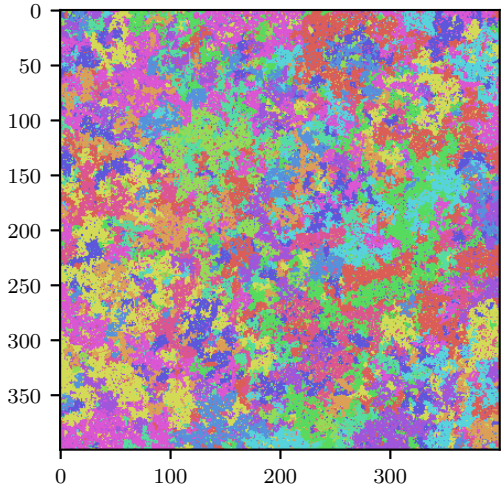

Figure 49: Example static-state of a SSM with 10% random condition.

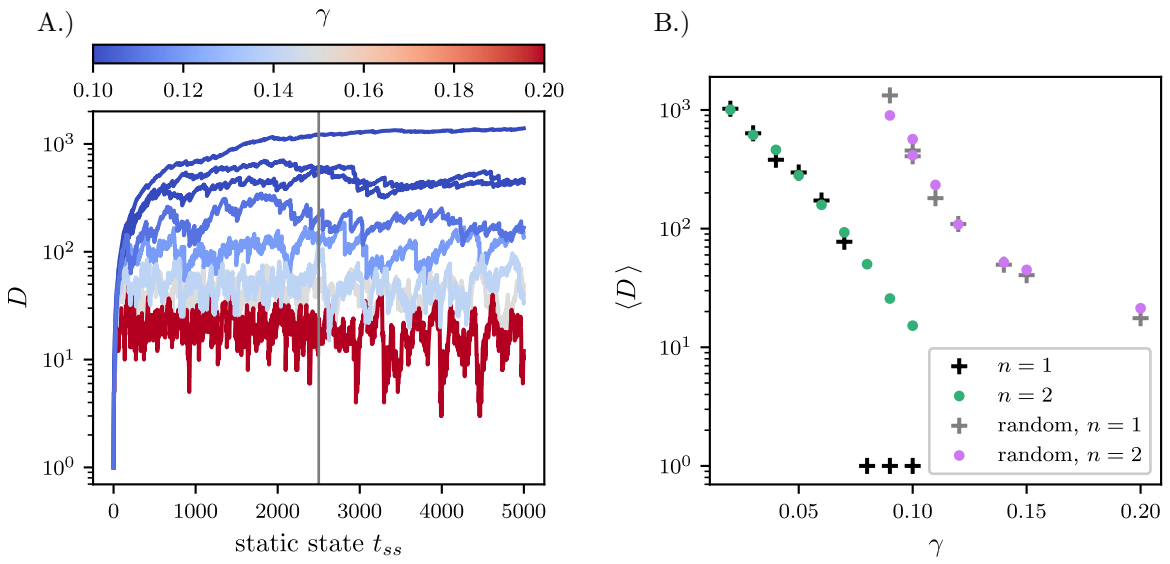

Figure 50: (A) Diversity time-series for system of size of size 400×400 and two randomly located conditions. (B) Average diversity for an unmodified SSM as well as the random-condition SSM. Both with $L = 400$.

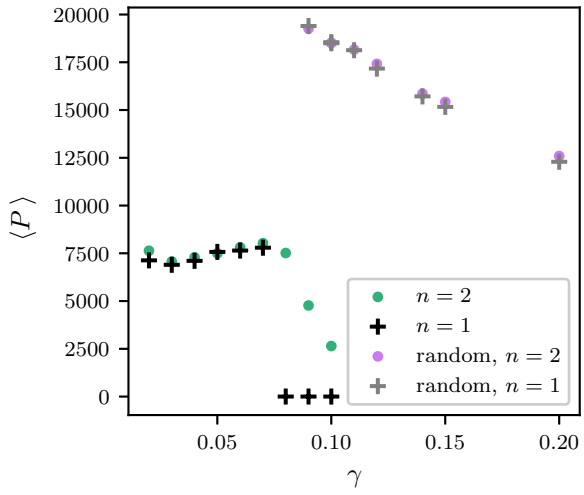

Figure 51: Average number of patches for the random-condition SSM and the unmodified version, both with $L = 400$.

The improvement in stability and increase in diversity are especially notable when the average diversity in figure (50.B) is considered. For both the building phase as well as the measurement-phase, comparable average diversities are achieved at significantly higher γ. Furthermore, since the system is able to recover from states of low diversity, the decline in average diversity seems to flatten off for higher γ. Figure (51) shows that the average number of patches decrease with γ. Furthermore, for the simulated values of γ it shows no sign of flattening off, unlike the other SSM models.

4.12 Removal of Cyclic Interactions

When the effect of cyclic interactions were first introduced in section 2.5, they were presented following [23]. There it was concluded that removal of short cycles in the interaction network increases the diversity in the system. This effect was visible for the removal of cycles of length ≤ 4. If larger cycles are removed as well, the system collapsed to its low diversity state with $D = 1$. The data for these conclusions was based on a systems with $L = 200$ and $\gamma \in \{0.05, 0.025\}$. These systems were initialized with a static state from a system random introduction rate $\alpha = 0.025$ and $\gamma = 0.05$. The appropriate graphic together with its original description are presented in figure (52).

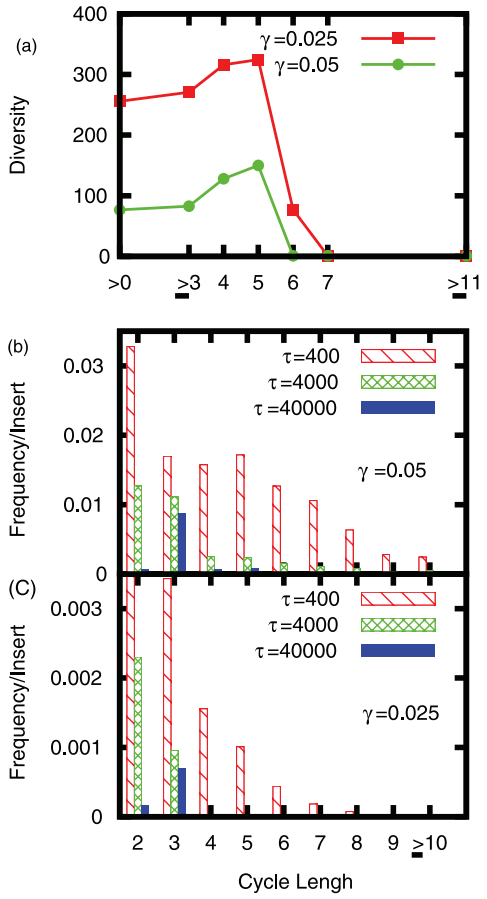

Figure 52: From [23]: "Quasistatic simulation of a system of size $L = 200$. (a) Diversity of a steady state short cycles of length below $2, 3, 4, \ldots$ are prevented from forming in the system. Removing cycles of length 2 is the same as allowing all cycles ≥ 3. The connecting lines are for guiding the the eye. (b), (c) Probability of having an active cycle of a certain length at time τ after the introduction of a new species for, respectively, (b) $\gamma = 0.05$ and (c) $\gamma = 0.025$. Notice that the probabilities do not add up to 1, which reflects the fact that the majority of new species does not activate a cyclic relation."

However, further analysis of the algorithm used for the generation of interaction-networks in these simulations could explain the increase in the diversity associated with the removal of cycles. This algorithm is defined as follows: when a new species is introduced, its interactions with other species are randomly chosen with probability γ. If any of these interactions would result in a cyclic interaction with length less than $C_{\min}$, the generated

interactions for the new species are discarded. This process repeats until suitable interactions are found.

While this algorithm succeeds in generating interaction networks of the desired cycle-structure, it can lead to significant differences for other network metrics. Most importantly, the number of edges $|E|$ is decreased. Ideally the network-generation should leave the chance of interacting with other species unchanged.

To show the impact on the network, the previously discussed algorithm was implemented and the data is displayed in figure (53). The maximum likelihood estimator of γ for the entire network ($\hat{\gamma}$) as well as the effective interaction probability for each node γ_{eff} are considered. It is clearly visible that higher choices of $C_{\min}$ result in lower $\hat{\gamma}$ and γ_{eff}. This effect increases as more nodes are added to the network.

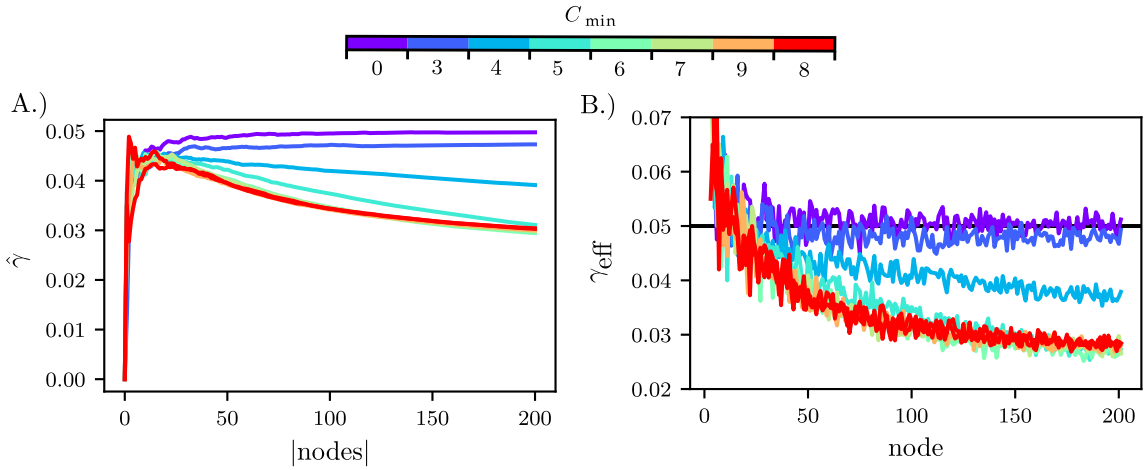

Figure 53: Effects of the the cycle removal algorithm on generated networks. A.) Maximum-likelihood estimator of γ as a function of network size. B.) Effective interaction probability γ_{eff} for each node of the network.

While the removal of species could reduce this effect to some extent, systems with higher diversity should be affected by it significantly. Due to time-constraints no further investigations were conducted; however, the decrease of introduced edges in the interaction-network gives a simple explanation for the increase in diversity displayed in figure (52).

5 Conclusions

5.1 Effects of System Size

Utilizing a parallel implementation with significantly improved simulation-speed for larger systems, the model of sessile species was simulated for system lengths L in $[200, 800]$ and interaction probabilities γ in $[0.01, 0.12]$. As expected, increases in system size show positive effects for the total diversity. Furthermore, larger systems allowed simulations with higher interaction probabilities to remain in their high-diversity state for the duration of the simulation.

Total diversity is found to grow linearly with lattice length L for a fixed value of γ (figure 36). The slope of this linear growth decreases, seemingly exponentially, with γ (figure 37). While higher interaction probabilities are found to produce more patches in the system (figure 38), they do not allow the system to speciate to the same extent, and therefore ultimately force the system to collapse to its low-diversity state.

5.2 Effects of Inhomogeneous Spatial Conditions

To investigate how inhomogeneous spatial conditions affect the SSM, three variations are discussed: the inactive-SSM (section 4.9), the split-SSM (section 4.10) and the random-condition SSM (section 4.11).

Out of these three, the sessile species model with inactive lattice sites showed the most similarity to the unmodified SSM. The diversity for higher interaction probabilities γ is slightly increased, whereas the number of patches is decreased (figure 41) and 42). The transition from the high-diversity state to the low-diversity state occurred at a slightly higher interaction probability.

In the split-SSM, boundaries between the two spatial conditions show clear, positive edge-effects as the transitional area has an increased number of patches (figure 46) and higher local diversity (figure 44). While a unmodified SSM of size 400×400 collapsed to its low-diversity state for interaction probabilities $\gamma \geq 0.07$, the split version of the same size did not collapse until $\gamma \geq 0.11$. This shows that a combined ecosystem can show different behaviour than its sub-ecosystems, both globally in regards to the collapse-threshold and the local edge-effects.

In comparison to the split-SSM, the random-condition SSM has longer boundaries in more complex shapes. As a result, the random-condition SSM is able to maintain a much higher diversity and number of patches (figure 50 and 51). Although the diversity did decrease as the interaction probability was increased, even the highest simulated interaction probability, $\gamma = 0.2$, did not force the random-condition SSM into a low diversity state.

In the unmodified sessile species model the fragmentation of the lattice into patches and the resulting spatial separation are achieved only by stochastic- and cyclic-patch creation. If spatial inhomogeneity is introduced into the model, spatial separation is increased further, as the spread of species is additionally hindered by spatial conditions. This added separation leads the discussed ecosystems of sessile species to develop higher diversities and improves their resistance to collapsing into a low-diversity state.

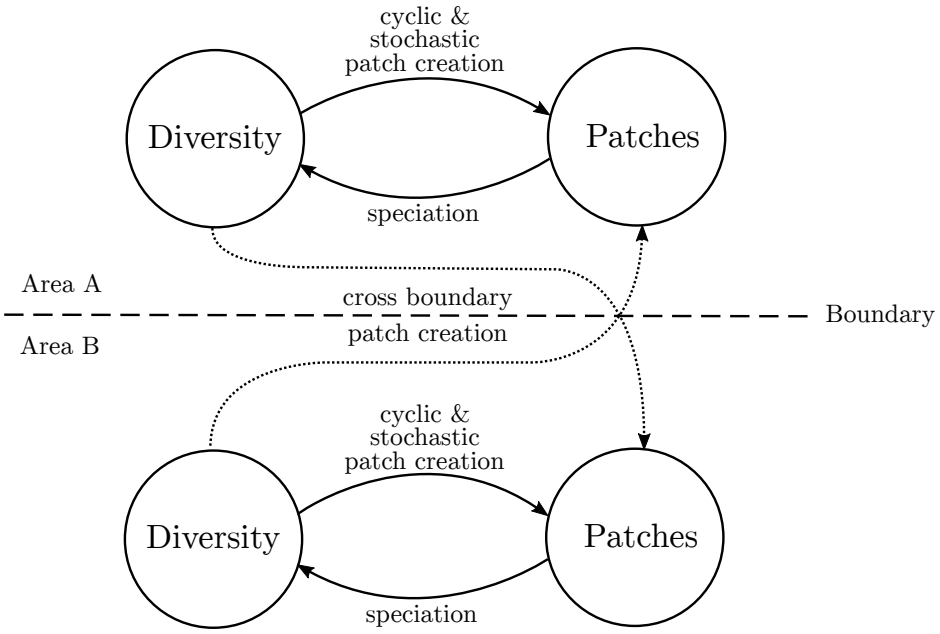

Figure 54: Illustration of two areas with different interactions interacting at a boundary. Isolated areas would only rely on the positive feedback-loop between their diversity and patches to remain in a high-diversity state. In the combined System, the species in area A could lead to cyclic and stochastic patch-creation in area B. These additionally patches would allow for more species to settle, increasing diversity in area B. As this process is symmetric an additional feedback loop is formed across the boundary.

6 References

1. Mathiesen, J., Mitarai, N., Sneppen, K. & Trusina, A. Ecosystems with Mutually Exclusive Interactions Self-Organize to a State of High Diversity. *Physical Review Letters* **107,** 188101. ISSN: 0031-9007. https://link.aps.org/doi/10.1103/PhysRevLett.107.188101 (Oct. 2011).
2. Ries, L. & Sisk, T. D. *A predictive model of edge effects* Nov. 2004. https://esajournals.onlinelibrary.wiley.com/doi/10.1890/03-8021%20http://doi.wiley.com/10.1890/03-8021.
3. Swan, P. *Lichen in the Lake District* https://www.istockphoto.com/photo/lichen-study-gm1156168122-315011581%20https://www.istockphoto.com/photo/salmonella-bacteria-gm874165142-244098604.
4. Lotka, A. J. Undamped oscillations derived from the law of mass action. *Journal of the American Chemical Society* **42,** 1595–1599. ISSN: 15205126 (1920).
5. Volterra, V. Fluctuations in the Abundance of a Species considered Mathematically. *Nature* **118,** 558–560. ISSN: 0028-0836. https://www.nature.com/articles/118558a0 (Oct. 1926).
6. Bacaër, N. *A Short History of Mathematical Population Dynamics* ISBN: 978-0-85729-114-1. http://link.springer.com/10.1007/978-0-85729-115-8 (Springer London, London, 2011).
7. Murray. *Mathematical Biology* (ed Murray, J. D.) ISBN: 978-0-387-95223-9. http://link.springer.com/10.1007/b98868 (Springer New York, New York, NY, 2002).
8. Gardner, M. R. & Ashby, W. R. Connectance of large dynamic (cybernetic) systems: critical values for stability. *Nature* **228,** 784. ISSN: 0028-0836. https://www.nature.com/articles/228784a0%20http://www.ncbi.nlm.nih.gov/pubmed/5472974 (Nov. 1970).
9. May, R. M. Will a large complex system be stable? *Nature* **238,** 413–414. ISSN: 00280836. https://www.nature.com/articles/238413a0 (Aug. 1972).
10. Allesina, S. & Grilli, J. in *Theoretical Ecology* 74–92 (Oxford University Press, May 2020). https://oxford.universitypressscholarship.com/view/10.1093/oso/9780198824282.001.0001/oso-9780198824282-chapter-6.

11. Gravel, D., Massol, F. & Leibold, M. A. Stability and complexity in model meta-ecosystems. *Nature communications* **7,** 12457. ISSN: 2041-1723. http://www.nature.com/articles/ncomms12457%20http://www.ncbi.nlm.nih.gov/pubmed/27555100%20http://www.pubmedcentral.nih.gov/articlerender.fcgi?artid=PMC4999499 (Nov. 2016).

12. Reichenbach, T., Mobilia, M. & Frey, E. Mobility promotes and jeopardizes biodiversity in rock–paper–scissors games. *Nature* **448,** 1046–1049. ISSN: 0028-0836. http://www.nature.com/articles/nature06095 (Aug. 2007).

13. Fernández, R., Louis, P.-Y. & Nardi, F. R. in, 1–30 (2018). https://doi.org/10.1007/978-3-319-65558-1_1%20http://link.springer.com/10.1007/978-3-319-65558-1_1.

14. Gardner, M. Mathematical Games. *Scientific American* **223,** 120–123. ISSN: 0036-8733. https://www.scientificamerican.com/article/mathematical-games-1970-10 (Oct. 1970).

15. Wolfram, S. Statistical mechanics of cellular automata. *Reviews of Modern Physics* **55,** 601–644. ISSN: 0034-6861. https://link.aps.org/doi/10.1103/RevModPhys.55.601 (July 1983).

16. Fuentes, M. A. & Kuperman, M. N. Cellular automata and epidemiological models with spatial dependence. *Physica A: Statistical Mechanics and its Applications* **267,** 471–486. ISSN: 03784371. www.elsevier.com/locate/physa%20https://linkinghub.elsevier.com/retrieve/pii/S0378437199000278 (May 1999).

17. Alves, S., Oliveira Neto, N. & Martins, M. Electoral surveys' influence on the voting processes: a cellular automata model. *Physica A: Statistical Mechanics and its Applications* **316,** 601–614. ISSN: 03784371. www.elsevier.com/locate/physa%20https://linkinghub.elsevier.com/retrieve/pii/S0378437102012086 (Dec. 2002).

18. Nagel, K., Wolf, D. E., Wagner, P. & Simon, P. Two-lane traffic rules for cellular automata: A systematic approach. *Physical Review E* **58,** 1425–1437. ISSN: 1063-651X. https://link.aps.org/doi/10.1103/PhysRevE.58.1425 (Aug. 1998).

19. Gilpin, M. E. Limit Cycles in Competition Communities. *The American Naturalist* **109,** 51–60. ISSN: 0003-0147. https://www.jstor.org/stable/2459636 (1975).

20. Jackson, J. B. C. & Buss, L. Alleopathy and spatial competition among coral reef invertebrates. *Proceedings of the National Academy of Sciences* **72,** 5160–5163. ISSN: 0027-8424. https://pnas.org/doi/full/10.1073/pnas.72.12.5160 (Dec. 1975).

21. Karlson, R. H. & Jackson, J. B. C. Competitive Networks and Community Structure: A Simulation Study. *Ecology* **62,** 670–678 (1981).

22. Karlson, R. H. & Buss, L. W. Competition, disturbance and local diversity patterns of substratum-bound clonal organisms: A simulation. *Ecological Modelling* **23,** 243–255. ISSN: 03043800. https://linkinghub.elsevier.com/retrieve/pii/0304380084901030 (June 1984).

23. Mitarai, N., Mathiesen, J. & Sneppen, K. Emergence of diversity in a model ecosystem. *Physical Review E - Statistical, Nonlinear, and Soft Matter Physics* **86,** 11929. ISSN: 15393755 (2012).

24. Mitarai, N., Heinsalu, E. & Sneppen, K. Speciation, diversification, and coexistence of sessile species that compete for space. *PLoS ONE* **9,** 96665. ISSN: 19326203. www.plosone.org (2014).

25. Uekermann, F., Mathiesen, J. & Mitarai, N. Characterization of phase transitions in a model ecosystem of sessile species. *Physical Review E* **95,** 032409. ISSN: 2470-0045. https://link.aps.org/doi/10.1103/PhysRevE.95.032409 (Mar. 2017).

26. Aerts, L. & van Soest, R. Quantification of sponge/coral interactions in a physically stressed reef community, NE Colombia. *Marine Ecology Progress Series* **148,** 125–134. ISSN: 0171-8630. http://www.int-res.com/abstracts/meps/v148/p125-134/ (1997).

27. St. Clair, L. *Crustose Lichens* https://www.fs.fed.us/wildflowers/beauty/lichens/gallery/crustose/index.shtml.

28. Lam, S. K., Pitrou, A. & Seibert, S. *Numba* in *Proceedings of the Second Workshop on the LLVM Compiler Infrastructure in HPC - LLVM '15* (ACM Press, New York, New York, USA, 2015), 1–6. ISBN: 9781450340052. http://dx.doi.org/10.1145/2833157.2833162.%20http://dl.acm.org/citation.cfm?doid=2833157.2833162.

29. *Release Notes — Numba* https://numba.readthedocs.io/en/stable/release-notes.html#version-0-54-0-19-august-2021.

30. Alstott, J., Bullmore, E. & Plenz, D. powerlaw: A Python Package for Analysis of Heavy-Tailed Distributions. *PLOS ONE* **9,** e85777. ISSN: 1932-6203. https://journals.plos.org/plosone/article?id=10.1371/journal.pone.0085777 (Jan. 2014).

7 Appendix

Average Diversities for $L = 252$ and $L = 800$

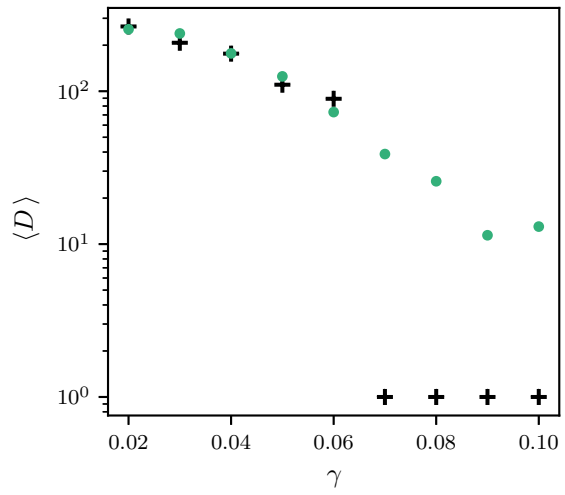

Figure 55: Average Diversity for a system of size 252×252 for various values of γ. The building phase is indicated by $n = 2$ and the measuring phase by $n = 1$

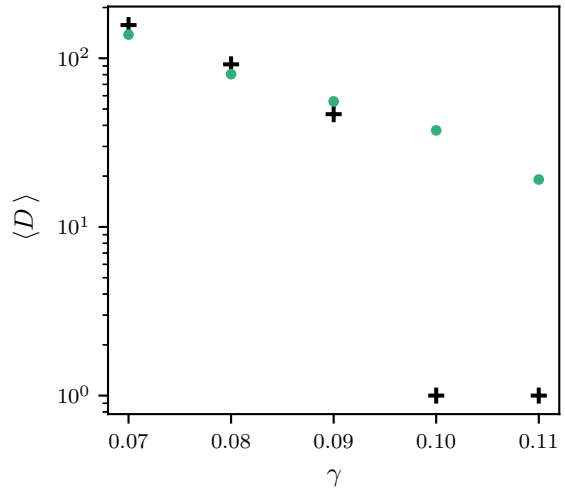

Figure 56: Average Diversity for a system of size 800×800 for various values of γ. The building phase is indicated by $n = 2$ and the measuring phase by $n = 1$

Species Size Distribution for $L = 252$ and $L = 800$ with $n_{intro} = 2$

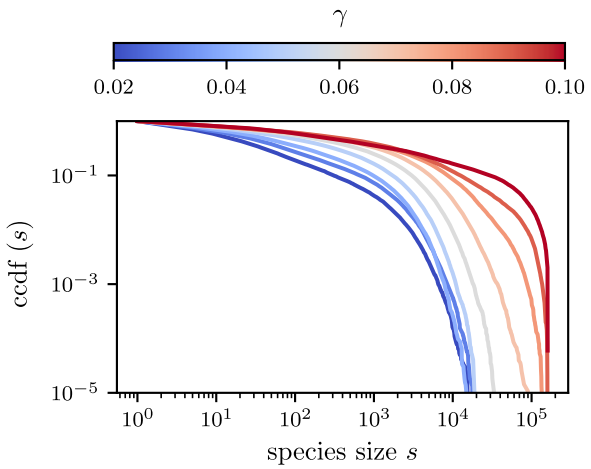

Figure 57: ccdf of species sizes for a system with $L = 252$ during its diversity building phase.

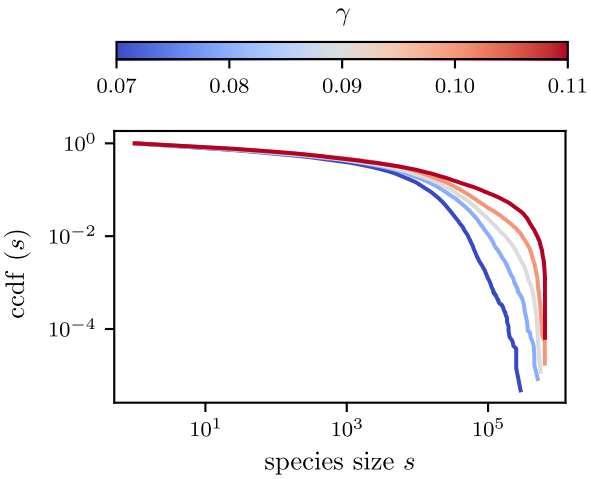

Figure 58: ccdf of species sizes for a system with $L = 800$ during its diversity building phase.

Patch Size Distribution for $L = 252$ and $L = 800$ with $n_{intro} = 2$

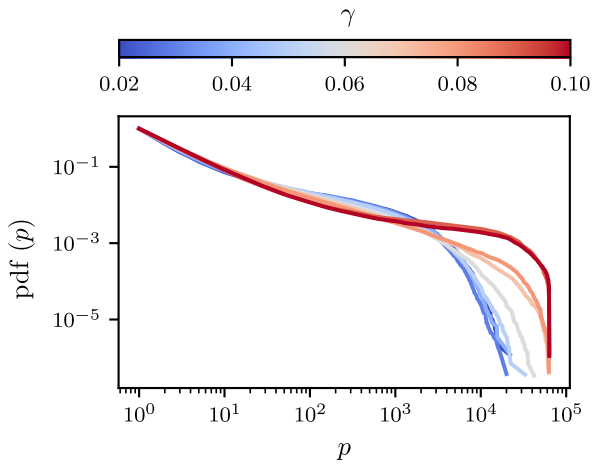

Figure 59: ccdf of patch sizes for a system with $L = 252$ during its diversity building phase.

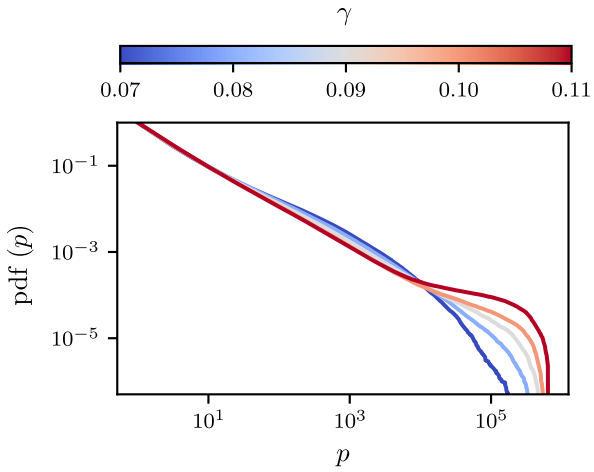

Figure 60: ccdf of patch sizes for a system with $L = 800$ during its diversity building phase.

Split-SSM of Size 800×800

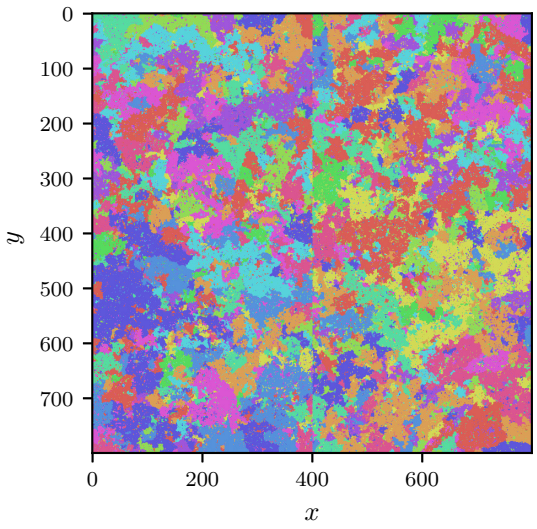

Figure 61: Example static-state of a split-SSM-ecosystem of size 800×800 and $\gamma = 0.06$. The boundary between the two areas with separate interaction networks is still visible at $x = 400$.

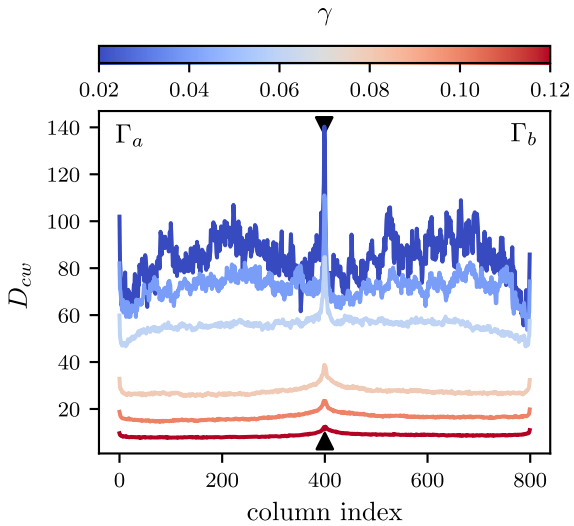

Figure 62: Column-wise diversity for various γ in a system of size 800×800. Only non-collapsing static states generated with $n_{\text{intro}} = 1$ are considered. Fewer γ were simulated, visually resulting in larger gaps between lines when compared to figure (44).